

# PASSIVE EARTH PRESSURE COEFFICIENT DURING EARTHQUAKE

MATSUHEI ICHIHARA\*, NOBUO MORI\*\*, SUSUMU NAKANE\*\*\*  
and ITSUO HIRANO\*\*\*\*

*Earth Pressure Research Laboratory*

(Received October 31, 1973)

## CONTENTS

1. Introduction
2. Calculation of Passive Earth Pressure during Earthquake by Means of Logarithmic Spiral Method
  - 2.1. Method of Calculation
  - 2.2. Calculation in the Case Where Sliding Surface is Convex
    - (1) Calculation of moment  $M_1$
    - (2) Calculation of moment  $M_2$
    - (3) Calculation of moment  $M_3$
    - (4) Calculation of moment  $M_4$
    - (5) Calculation of arm length  $l_0$  of resultant force  $P_{PE}$  from spiral center
  - 2.3. Calculation in the Case Where Sliding Surface is Concave
    - (1) Calculation of moment  $M_1$
    - (2) Calculation of moment  $M_2$
    - (3) Calculation of moment  $M_3$
    - (4) Calculation of moment  $M_4$
    - (5) Calculation of arm length  $l_0$  of  $P_{PE}$  from spiral center
  - 2.4. Passive Earth Pressure on Vertical Section and Angle at Which Sliding Surface Intersects with Backfill Surface
3. Calculation of Passive Earth Pressure during Earthquake by the Sokolovski Method
4. Comparison of Results by the Logarithmic Spiral Method and by Other Method
  - 4.1. Coefficient  $K_{PE}$  of Passive Earth Pressure
    - (1) The case of  $\delta=0^\circ$
    - (2) The case of  $\delta=\pm\frac{1}{2}\phi$  and  $\delta=\frac{2}{3}\phi$
    - (3) The case of  $\delta=\phi$
  - 4.2. Sliding Surface
    - (1) Relationship between sliding surface, angle of wall friction and angle of internal friction
    - (2) Relationship between sliding surface and seismic force
    - (3) Relationship between sliding surface and inclination of ground surface
    - (4) Relationship between sliding surface and inclined angle of wall
    - (5) Comparison between sliding surface of the spiral method and that of the Sokolovski method
  - 4.3. Comparison between the Author's Results, Mayer-Vorfelder's Ones and Terzaghi's Ones
5. Conclusions

---

\* Professor, Earth Pressure Research Laboratory

\*\* Engineer, Shimizu Construction Co., Ltd.

\*\*\* Research Assistant, Earth Pressure Research Laboratory

\*\*\*\* Graduate Student

## Appendix

1. Monobe Equation
2. Accuracy of Calculation
3. Passive Earth Pressure of Cohesive Soils and Passive Earth Pressure of Soils under Uniform Surcharge
4. Tables

## 1. Introduction

The calculation of the passive earth pressure is very important to know the stability of the retaining walls and the ultimate bearing capacity of foundations. This calculation of the passive earth pressure is more difficult than that of the active earth pressure, because the sliding surface of passive earth pressure is clearly curved in difference with the case of active earth pressure.

Therefore, the authors calculated the coefficients of passive earth pressure and obtained the detailed tables of them by assuming the curved sliding surface which is more realistic than the straight line of sliding.

The studies on this problem in the static state have been made since earlier time. Kötter (1888)<sup>1)</sup>, Müller-Breslau (1906)<sup>2)</sup>, Reissner (1909)<sup>2)</sup>, Anzo (1949)<sup>3)</sup> *et al.* studied this problem considering plastic equilibrium. It was reported that Schwelder (1887)<sup>2)</sup> studied firstly the passive earth pressure by assuming the sliding surface as the logarithmic spiral. Kármán (1926)<sup>4)</sup> obtained the shapes of sliding surfaces and the coefficients of active earth pressure by substituting the Mohr-Coulomb criterion into the equilibrium equations, and expanding these results into infinite serieses. His work was remarkable on the assumption that the wall friction was equal to the internal friction of soil. His method can also be used for the calculation of the passive earth pressure. Fellenius (1927)<sup>1)2)</sup> considered firstly that the passive earth pressure was the minimum value of assumed lateral pressure of the circular sliding surface. His method has been utilized in the case of cohesive soil. Krey (1936)<sup>5)</sup> and Ohde (1938)<sup>2)6)</sup> analyzed the problem of the passive earth pressure by assuming that the sliding surface consisted of a logarithmic spiral and a straight line. Caquot and Kerisel (1949)<sup>7)</sup> studied the stress components in the soil mass with the finite difference method and published tables of the coefficients of passive earth pressure.

Later, Sokolovski (1960)<sup>8)</sup> studied the problem of the earth pressure and the bearing capacity of foundations and gave the tables of coefficients of earth pressure, solving Karman's Equation by use of the finite difference method. Recently, Mayer-Vorfelder (1970)<sup>2)</sup> obtained the detailed tables of coefficients of passive earth pressure in the case of internal friction  $\phi=40^\circ$ , assuming that the sliding surface consisted of a logarithmic spiral and a straight line.

Although many studies were performed, the coefficients of passive earth pressure during earthquake have not been studied. Therefore, the authors obtained here them with assuming that the sliding surface consisted of a logarithmic spiral and a straight line, and also with extending the Sokolovski method. The Sokolovski method is superior to the logarithmic spiral method from the point of view of the equilibrium of soil mass above the sliding surface and the boundary condition at the point of contact between the wall and the sliding surface. In this paper, the authors assumed many cases of the wall friction and the shape of wall, and compared the coefficients  $K_{PE}$  of passive earth pressure

during earthquake between the logarithmic spiral method, the Sokolovski method and the Mononobe method (see Appendix 1). It has become clear that the difference in the results of these methods increased with increasing in the angle of wall friction, with increasing in the inclination of the back face of wall and with increasing in the inclination of ground surface.

**2. Calculation of Passive Earth Pressure during Earthquake by Means of Logarithmic Spiral Method**

*2.1. Method of Calculation*

The passive earth pressure indicates the resistance of soil mass against the wall which is displaced toward the soil mass. This pressure is utilized to know the support of soil mass for structures such as retaining walls or sheet pile walls. The following computation is based on the assumption that the wall is moved toward the backfill soil during earthquake and that the shape of sliding surface BD in Fig. 1 is given by a logarithmic spiral, and DC is given by a straight line. The seismic force is treated as positive when it acts toward the backfill from the wall.

Within the soil mass of  $\triangle ADC$ , the state of stresses is the same as the passive Rankine pressure acting on the vertical section DF under earthquake. The straight line AD is  $+m$  sliding surface and DC is  $-m$  sliding surface as shown in Fig. 1. If the center of the logarithmic spiral O is located on the upper extension line of AD, the sliding surface BC is convex surface. On the other hand, BD is a concave surface when the center O is located on the lower extension line of AD as shown in Fig. 2.

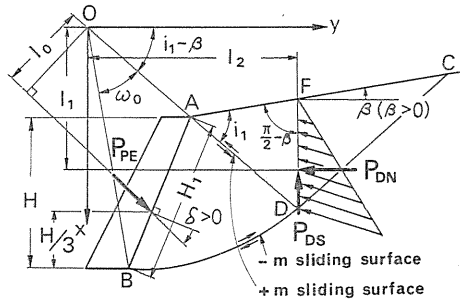


FIG. 1. Sliding surface of convex logarithmic spiral curve.

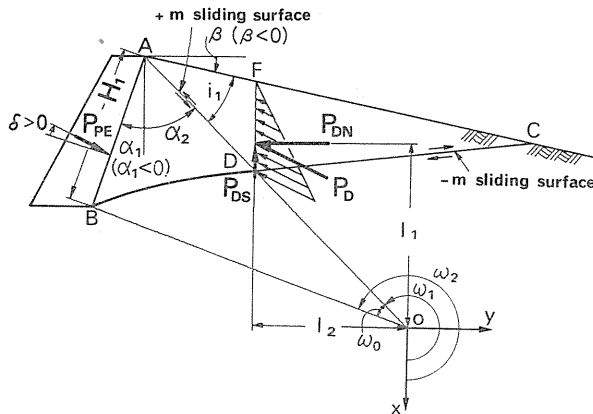


FIG. 2. Sliding surface of concave logarithmic spiral curve.

In the both figures, the sliding surface DC is tangent to the curved surface BD. Since the resultant reaction  $R$  along the curved section BD passes through the center O, the moment  $M$  of passive earth pressure  $P_{PE}$  during earthquake about the center O must be equal to the total moment of the gravity force of soil ABDF, the seismic force acting on the soil mass ABDF and the force acting on the vertical section FD during earthquake.

And the next equations are obtained for Fig. 1 and Fig. 2 respectively;

$$P_{PE} \cdot l_0 = -M_1 + M_2 + M_3 + M_4, \quad (1)$$

$$P_{PE} \cdot l_0 = M_1 - M_2 + M_3 + M_4. \quad (2)$$

where  $l_0$ : the arm length of the resultant force of pressure  $P_{PE}$  from the center of spiral,

$M_1$ : the moment about the center O of spiral by the body force including seismic effect of assumed soil mass of  $\triangle OBA$ ,

$M_2$ : the moment about the center O by the body force including seismic effect of assumed soil mass of sector OBD,

$M_3$ : the moment about the center O by the body force including seismic effect of soil mass of  $\triangle ADF$ , and

$M_4$ : the moment about the center O by the passive Rankine earth pressure including seismic effect acting upon the vertical section FD;

$$M_4 = l_1 \cdot P_{DN} + l_2 \cdot P_{DS}. \quad (3)$$

In Eq. 3,  $P_{DN}$  is the normal resultant force acting on the vertical section FD, and  $P_{DS}$  is the shear force acting along the section FD. The force  $P_{DN}$  is positive. In Fig. 1 and Fig. 2, the force  $P_{DS}$  is considered negative when it acts upward. The lengths of  $l_1$  and  $l_2$  are the arms of two forces of  $P_{DN}$  and  $P_{DS}$  from the spiral center O respectively.

In the following investigation, it will be assumed that the origin of the  $X$ - $Y$  coordinates is situated on the spiral center O as shown in Fig. 1. The passive earth pressure during earthquake can be determined by the minimum value  $P_{PE}$  which is calculated with Eq. 1 or Eq. 2. Hence, the passive earth pressure during earthquake is determined with the following equation;

$$P_{PE} = \frac{1}{2} \gamma H_1^2 \cos \alpha_1 \frac{K_{PE}}{\cos \delta}, \quad (4)$$

where  $H_1$ : the length of the back face of wall,

$\gamma$ : unit weight of backfill,

$\alpha_1$ : the angle of the backface of wall from vertical plane

$\delta$ : the angle of wall friction and

$K_{PE}$ : the coefficient of the passive earth pressure during earthquake.

The value of  $\alpha_1$  is considered positive if the backface of wall is inclined to the right as shown in Fig. 3 (a). If  $\gamma$  equals 1.0, equation 4 becomes Eq. 5;

$$K_{PE} = \frac{2 P_{PE} \cos \delta}{H_1^2 \cos \alpha_1}. \quad (5)$$

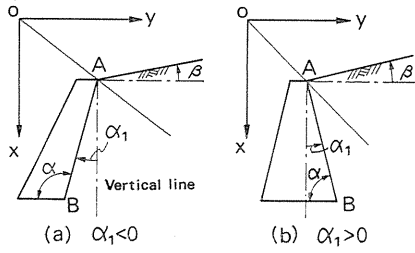


FIG. 3. Inclined angle of the backface of wall.

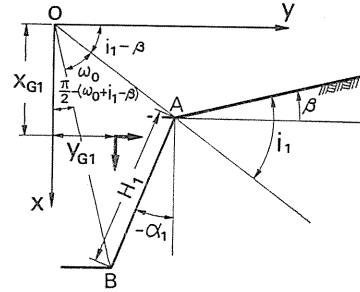


FIG. 4. Determination of side lengths of  $\triangle OBA$ .

2.2. Calculation in the Case Where Sliding Surface is Convex

Substituting the following equation into Eq. 1, the resultant force of passive earth pressure can be given by the minimum value of  $P_{PE}$  for various values of  $\omega_0$  which is shown in Fig. 1.

(1) Calculation of moment  $M_1$

The side lengths of  $\triangle OBA$  are given by the following equations;

$$\left. \begin{aligned} \overline{AB} &= H_1, \\ \overline{OA} &= \frac{\cos(\omega_0 + i_1 - \beta + \alpha_1)}{\sin \omega_0} \cdot H_1, \\ \overline{OB} &= \frac{\cos(\beta - i_1 - \alpha_1)}{\sin \omega_0} \cdot H_1, \end{aligned} \right\} \quad (6)$$

where  $H_1$ : the length of backface of wall,

$\beta$ : the inclined angle of backfill surface from the horizontal, and

$i_1, \omega_0$ : the angles shown in Fig. 4.

Then, the coordinates  $(x, y)$  of edge points of  $\triangle OBA$  are as follows;

$$O: (0, 0),$$

$$A: (\overline{OA} \sin(i_1 - \beta), \overline{OA} \cos(i_1 - \beta)),$$

$$B: (\overline{OB} \sin(\omega_0 - \beta + i_1), \overline{OB} \cos(\omega_0 - \beta + i_1)).$$

The coordinates  $(x_{G1}, y_{G1})$  of the center of gravity in  $\triangle OBA$  are as follows;

$$x_{G1} = \frac{1}{3} \left[ \overline{OA} \sin(i_1 - \beta) + \overline{OB} \sin(\omega_0 - \beta + i_1) \right],$$

$$y_{G1} = \frac{1}{3} \left[ \overline{OA} \cos(i_1 - \beta) + \overline{OB} \cos(\omega_0 - \beta + i_1) \right].$$

The area  $S_{OBA}$  of  $\triangle OBA$  is given by the following equation;

$$S_{OBA} = \frac{1}{2} \overline{OA} \cdot \overline{OB} \sin \omega_0.$$

In conclusion,  $M_1$  is represented by Eq. 7;

$$M_1 = S_{OBA}(y_{G1} - \tan \theta_0 \cdot x_{G1}), \quad (7)$$

where  $\theta_0$  is given by Eq. 27.

(2) Calculation of moment  $M_2$

The sliding surface BD in Fig. 1 is given by the following logarithmic spiral equation;

$$r = r_0 e^{\omega \cdot \tan \phi}, \quad (8)$$

where  $r$ : the length of vector shown in Fig. 5,  
 $r_0$ : the length of vector  $r$  for  $\omega=0$ ,  
 $e$ : base of natural logarithm, and  
 $\omega$ : the angle of vector  $r$  from  $r_0$  (expressed in radians), and  $\omega$  is positive when it is measured counterclockwise.

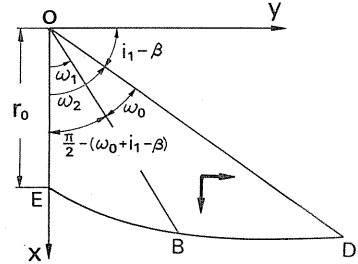


FIG. 5. Determination of moment  $M_2$  of the spiral method (convex downward).

The moment  $M_2$  is given by the next equation;

$$M_2 = M_x - M_y, \quad (9)$$

where 
$$M_x = \int y dA = \int_{\omega_1}^{\omega_2} \frac{2}{3} r \cdot \sin \omega \cdot \frac{1}{2} r^2 d\omega = \frac{1}{3} \int_{\omega_1}^{\omega_2} r^3 \sin \omega d\omega.$$

Accordingly, the moments  $M_x$  and  $M_y$  are represented by the following equations;

$$\left. \begin{aligned} M_x &= \frac{1}{3} r_0^3 \frac{1}{1+9 \tan^2 \phi} [e^{3 \omega \cdot \tan \phi} (3 \tan \phi \sin \omega - \cos \omega)]_{\omega_1}^{\omega_2} \\ M_y &= \frac{1}{3} r_0^3 \frac{1}{1+9 \tan^2 \phi} [e^{3 \omega \cdot \tan \phi} (3 \tan \phi \cos \omega + \sin \omega)]_{\omega_1}^{\omega_2} \end{aligned} \right\} \quad (10)$$

In the above equations, the values of  $\omega_1$ ,  $\omega_2$  and  $r_0$  are as follows;

$$\left. \begin{aligned} \omega_1 &= \angle EOB \text{ in Fig. 5} = \frac{\pi}{2} - (\omega_0 + i_1 - \beta), \\ \omega_2 &= \angle EOD \text{ in Fig. 5} = \frac{\pi}{2} - (i_1 - \beta), \end{aligned} \right\} \quad (11)$$

$$r_0 = \frac{\cos(\beta - i_1 - \alpha_1)}{\sin \omega_0} \cdot H_1 \cdot e^{(\omega_0 + i_1 - \beta - \pi/2) \cdot \tan \phi}. \quad (12)$$

(3) Calculation of moment  $M_3$

In Fig. 1, the lengths  $\overline{AD}$  and  $\overline{OD}$  are as follows;

$$\left. \begin{aligned} \overline{AD} &= \overline{OD} - \overline{OA}, \\ \overline{OD} &= \overline{OB} \cdot e^{\omega_0 \tan \phi} = \frac{\cos(\beta - i_1 - \alpha_1)}{\sin \omega_0} H_1 \cdot e^{\omega_0 \tan \phi}. \end{aligned} \right\} \quad (13)$$

where  $\overline{OA}$  is given by Eq. 6.

Accordingly, the side lengths of  $\triangle ADF$  are as follows;

$$\begin{aligned}\overline{AD} &= [\cos(\beta - i_1 - \alpha_1)e^{\omega_0 \cdot \tan \beta} - \cos(\omega_0 + i_1 - \beta + \alpha_1)] \frac{H_1}{\sin \omega_0} \\ \overline{AF} &= \frac{\cos(i_1 - \beta)}{\cos \beta} \overline{AD}, \text{ and} \\ \overline{FD} &= \frac{\sin i_1}{\cos \beta} \overline{AD}.\end{aligned}$$

The coordinates  $(x, y)$  of three vertexes of  $\triangle ADF$  are as follows;

$$\begin{aligned}A &: [\overline{OA} \sin(i_1 - \beta), \overline{OA} \cos(i_1 - \beta)], \\ D &: [\overline{OD} \sin(i_1 - \beta), \overline{OD} \cos(i_1 - \beta)], \text{ and} \\ F &: [\overline{OD} \sin(i_1 - \beta) - \overline{FD}, \overline{OD} \cos(i_1 - \beta)].\end{aligned}$$

The coordinates  $(x_{G3}, y_{G3})$  of the center of gravity of  $\triangle ADF$  are as follows;

$$\begin{aligned}x_{G3} &= \frac{1}{3} [(2\overline{OD} + \overline{OA}) \sin(i_1 - \beta) - \overline{FD}], \\ y_{G3} &= \frac{1}{3} [(2\overline{OD} + \overline{OA}) \cos(i_1 - \beta)].\end{aligned}$$

The area  $S_{ADF}$  of  $\triangle ADF$  is given by the following equation;

$$\begin{aligned}S_{ADF} &= \frac{1}{2} \cdot \overline{AD} \cdot \overline{AF} \sin i_1 \\ &= \frac{1}{2} \overline{AD}^2 \frac{\cos(i_1 - \beta)}{\cos \beta} \cdot \sin i_1.\end{aligned}$$

In conclusion,  $M_3$  is obtained by Eq. 14;

$$M_3 = S_{ADF} (y_{G3} - \tan \theta_0 \cdot x_{G3}). \quad (14)$$

(4) Calculation of moment  $M_4$

The moment  $M_4$  is already given by Eq. 3. The arm lengths of  $l_1$  and  $l_2$  in Fig. 1 are as follows;

$$\left. \begin{aligned}l_1 &= \overline{OD} \sin(i_1 - \beta) - \frac{1}{3} \overline{FD}, \text{ and} \\ l_2 &= \overline{OD} \cos(i_1 - \beta).\end{aligned} \right\} \quad (15)$$

The length  $\overline{OD}$  is given by Eq. 13. The normal force  $P_{DN}$  and the shearing force  $P_{Ds}$  are given in the next section.

(5) Calculation of arm length  $l_0$  of resultant force  $P_{PE}$  from spiral center

The applied point of the resultant force of passive earth pressure on the wall AB is at the height of  $H/3$  above B as shown in Fig. 1. Referring Fig. 6,  $l_0$  is obtained by the following equation;

$$l_0 = (\overline{OB} - \overline{BB'}) \sin(\omega_0 + i_1 - \beta + \alpha_1 - \delta) \quad (16)$$

where  $\overline{BB'} = \frac{1}{3} H_1 \frac{\cos \delta}{\sin(\omega_0 + i_1 - \beta + \alpha_1 - \delta)}$ ,

$\overline{OB}$  is given by Eq. 6.

2.3. Calculation in the Case Where Sliding Surface is Concave

Substituting the following equations into Eq. 2, the resultant force of passive earth pressure can be given by the minimum value of  $P_{PE}$  for various values of  $\omega_0$  which is shown in Fig. 2.

(1) Calculation of moment  $M_1$

In Fig. 2 where  $\beta < 0$ , the side lengths of  $\triangle ABO$  are obtained by the following equations;

$$\left. \begin{aligned} \overline{AB} &= H_1 \\ \overline{AO} &= \frac{\cos(i_1 - \beta + \alpha_1 - \omega_0)}{\sin \omega_0} H_1, \text{ and} \\ \overline{BO} &= \frac{\cos(i_1 - \beta + \alpha_1)}{\sin \omega_0} H_1. \end{aligned} \right\} \quad (17)$$

Then, the coordinates  $(x_{G1}, y_{G1})$  of the center of gravity of  $\triangle ABO$  are as follows;

$$\begin{aligned} x_{G1} &= -\frac{1}{3} [\overline{AO} \sin(i_1 - \beta) + \overline{BO} \sin(i_1 - \beta - \omega_0)], \text{ and} \\ y_{G1} &= -\frac{1}{3} [\overline{AO} \cos(i_1 - \beta) + \overline{BO} \cos(i_1 - \beta - \omega_0)]. \end{aligned}$$

The area  $S_{ABO}$  of  $\triangle ABO$  is given by the following equation;

$$S_{ABO} = \frac{1}{2} \cdot \overline{AO} \cdot \overline{BO} \sin \omega_0$$

Therefore,  $M_1$  is obtained by Eq. 18.

$$M_1 = S_{ABO} (|y_{G1}| - \tan \theta_0 \cdot |x_{G1}|). \quad (18)$$

(2) Calculation of moment  $M_2$

The sliding surface  $BD$  of logarithmic spiral is expressed by Eq. 8 and the moment  $M_2$  is given by Eq. 9 and Eq. 10.

In order to calculate  $M_2$ , the values of  $\omega_1$ ,  $\omega_2$  and  $r_0$  shown in Fig. 7 are obtained by the following equations;

$$\left. \begin{aligned} \omega_1 &= \frac{3\pi}{2} - i_1 + \beta, \\ \omega_2 &= \frac{3\pi}{2} - i_1 + \beta + \omega_0, \text{ and} \\ r_0 &= \frac{\cos(i_1 - \beta + \alpha_1)}{\sin \omega_0} H_1 \cdot e^{(i_1 - \beta - \omega_0 - 3\pi/2) \tan \phi} \end{aligned} \right\} \quad (19)$$

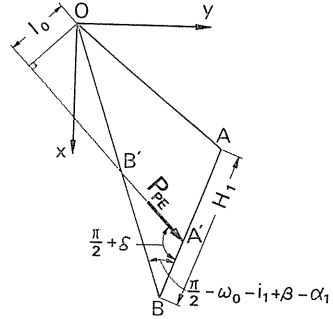


FIG. 6. Determination of the arm length  $l_0$  of  $P_{PE}$  from the spiral center  $O$  (convex downward).

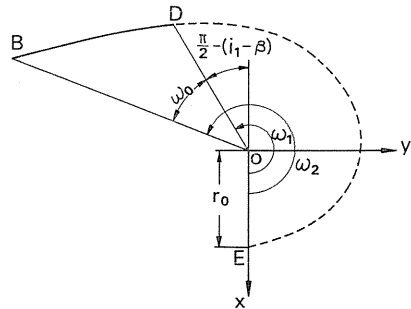


FIG. 7. Determination of moment  $M_2$  of the spiral method (concave downward).



(3) Calculation of moment  $M_3$

In Fig. 2, the side lengths of  $\triangle ADF$  are given by the following equations;

$$\left. \begin{aligned} \overline{FD} &= \frac{\sin i_1}{\cos \beta} \overline{AD}, \\ \overline{AF} &= \frac{\cos(i_1 - \beta)}{\cos \beta} \overline{AD}, \text{ and} \\ \overline{AD} &= \overline{AO} - \overline{DO}. \end{aligned} \right\} \quad (20)$$

where  $\overline{AO}$  is given by Eq. 6 and  $\overline{DO}$  is given by the following equation;

$$\overline{DO} = \frac{\cos(i_1 - \beta + \alpha_1)}{\sin \omega_0} H_1 \cdot e^{-\omega_0 \tan \beta} \quad (21)$$

The center of gravity of  $\triangle ADF$  is represented by the following coordinates ( $x_{G3}$ ,  $y_{G3}$ );

$$\begin{aligned} x_{G3} &= -\frac{1}{3} [(\overline{AO} + 2\overline{DO}) \sin(i_1 - \beta) + \overline{FD}], \text{ and} \\ y_{G3} &= -\frac{1}{3} (\overline{AO} + 2\overline{DO}) \cos(i_1 - \beta). \end{aligned}$$

The area  $S_{ADF}$  of  $\triangle ADF$  is given as follows;

$$S_{ADF} = \frac{1}{2} \overline{AD}^2 \frac{\cos(i_1 - \beta)}{\cos \beta} \sin i_1.$$

Therefore,  $M_3$  is given by the following equation;

$$M_3 = S_{ADF} (|y_{G3}| - \tan \theta_0 |x_{G3}|). \quad (22)$$

(4) Calculation of moment  $M_4$

In Fig. 2, the arm lengths of  $l_1$  and  $l_2$  are obtained by the following equations;

$$\left. \begin{aligned} l_1 &= \overline{DO} \sin(i_1 - \beta) + \frac{1}{3} \overline{FD}, \\ l_2 &= \overline{DO} \cos(i_1 - \beta). \end{aligned} \right\} \quad (23)$$

In the above equations, the length  $\overline{DO}$  is given by Eq. 21.

(5) Calculation of arm length  $l_0$  of  $P_{PE}$  from spiral center

Referring Fig. 8,  $l_0$  is obtained by the following equation;

$$l_0 = \overline{OA'} \sin(i_1 - \beta + \alpha_1 - \delta). \quad (24)$$

where  $\overline{OA'} = \overline{OA} - \overline{A'A}$ ,

$$\overline{A'A} = \frac{2}{3} H_1 \frac{\cos \delta}{\sin(i_1 - \beta + \alpha_1 - \delta)}, \text{ and}$$

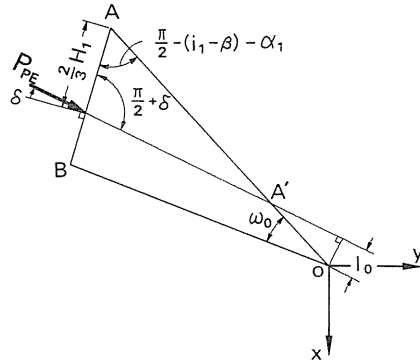


FIG. 8. Determination of the arm length  $l_0$  of  $P_{PE}$  (concave downward).

$$\overline{OA} = \frac{\cos(i_1 - \beta + \alpha_1 - \omega_0)}{\sin \omega_0} \cdot H_1.$$

2.4. *Passive Earth Pressure on Vertical Section and Angle at Which Sliding Surface Intersects with Backfill Surface*

In order to discuss stresses and sliding surface in the Rankine region during earthquake, we use the rectangular coordinates ( $u, v$ ) and ( $x, y$ ) as shown in Fig. 9. The stress components  $\sigma_u$  and  $\tau_{uv}$  of body force including seismic effect of soil mass acting on the  $u$ -plane are given by the following equations;

$$\left. \begin{aligned} \sigma_u &= \gamma_0 u \cos \beta_0, \\ \tau_{uv} &= -\gamma_0 u \sin \beta_0. \end{aligned} \right\} \quad (25)$$

In Eq. 25,  $\gamma_0$  and  $\beta_0$  are given by Eq. 26.

$$\left. \begin{aligned} \gamma_0 &= \frac{\gamma}{\cos \theta_0}, \\ \beta_0 &= \beta - \theta_0. \end{aligned} \right\} \quad (26)$$

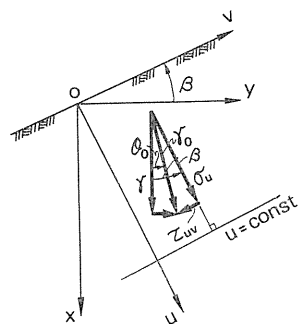


FIG. 9. Stress in the Rankine region during earthquake.

where  $\theta_0$  is defined with the horizontal acceleration of earthquake,  $a$ , and with the acceleration of gravity force,  $g$ , as follows;

$$\theta_0 = \tan^{-1} a/g. \quad (27)$$

In the plastic equilibrium state, the stress components  $\sigma_u, \sigma_v$  and  $\tau_{uv}$  can be expressed in terms of two variables  $\tilde{\sigma}$  and  $\phi_1$ ;

$$\left. \begin{aligned} \sigma_u &= \tilde{\sigma}(1 + \sin \phi \cos 2\phi_1), \\ \sigma_v &= \tilde{\sigma}(1 - \sin \phi \cos 2\phi_1), \text{ and} \\ \tau_{uv} &= -\tilde{\sigma} \sin \phi \sin 2\phi_1. \end{aligned} \right\} \quad (28)$$

where  $\sigma_v$  is stress component acting on the  $v$ -plane,  $\tilde{\sigma}$  is obtained by the Mohr circle corresponding to passive state in earthquake condition as shown in Fig. 10, and

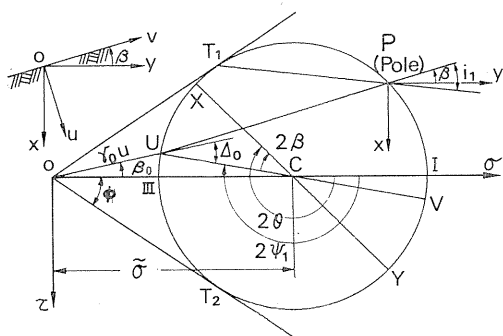


FIG. 10. Mohr's diagram in passive state during earthquake.

$\phi_1$  is angle between  $u$ -plane and major principal plane, and considered positive when it is measured counterclockwise from major principal plane.

We obtain the following equation from Eq. 25 and Eq. 28.

$$\sin(2\phi_1 - \beta_0) - \sin \Delta_0 = 0. \quad (29)$$

where

$$\left. \begin{aligned} \sin \Delta_0 &= \frac{\sin \beta_0}{\sin \phi} \quad \text{and} \\ |\Delta_0| &\leq \frac{\pi}{2}. \end{aligned} \right\} \quad (30)$$

Accordingly,  $\phi_1$  is represented by the following equation.

$$2\phi_1 = \beta_0 - \Delta_0 - \pi. \quad (31)$$

Further, equating  $\tau_{uv}$  of Eq. 25 and  $\tau_{uv}$  of Eq. 28, we obtain the following equation;

$$\tilde{\sigma} = \gamma_0 u \frac{\sin \Delta_0}{\sin 2\phi_1}.$$

The normal stress  $\sigma_y$  and the shearing stress  $\tau_{yx}$  at  $y=0$  are given by the following equations;

$$\left. \begin{aligned} \sigma_y &= \tilde{\sigma} [1 + \sin \phi \cos(\beta + \theta_0 + \Delta_0)] \quad \text{and} \\ \tau_{yx} &= -\tau_{xy} = \tilde{\sigma} \sin \phi \sin(\beta + \theta_0 + \Delta_0). \end{aligned} \right\} \quad (32)$$

where

$$\tilde{\sigma} = \frac{\gamma x \cos \beta}{\cos^2 \phi \cos \theta_0} (\cos \beta_0 + \sqrt{\cos^2 \beta_0 - \cos^2 \phi}).$$

Therefore,  $P_{DN}$  and  $P_{DS}$  are obtained by the following equations;

$$\left. \begin{aligned} P_{DN} &= \frac{1}{2} \overline{FD} \sigma_y \quad (x = FD) \\ &= \frac{\gamma \overline{FD}^2 \cos \beta}{2 \cos^2 \phi \cos \theta_0} [1 + \sin \phi \cos(\beta + \theta_0 + \Delta_0)] (\cos \beta_0 + \sqrt{\cos^2 \beta_0 - \cos^2 \phi}), \\ P_{DS} &= \frac{1}{2} \overline{FD} \tau_{yx} \quad (x = FD) \\ &= \frac{\gamma \overline{FD}^2 \cos \beta}{2 \cos^2 \phi \cos \theta_0} \sin \phi \sin(\beta + \theta_0 + \Delta_0) (\cos \beta_0 + \sqrt{\cos^2 \beta_0 - \cos^2 \phi}). \end{aligned} \right\} \quad (33)$$

As above mentioned, the sliding surface AD is  $+m$  sliding surface in Fig. 1 and Fig. 2. The pole of the Mohr circle in Fig. 10 is the intersection between the Mohr circle and the line which is parallel to the  $v$ -axis from the stress point  $U$ . The direction of  $+m$  sliding surface can be given by the straight line  $PT_1$ . The angle  $i_1$  between the backfill surface and the sliding surface AD can be obtained in Fig. 10 and expressed as follows;

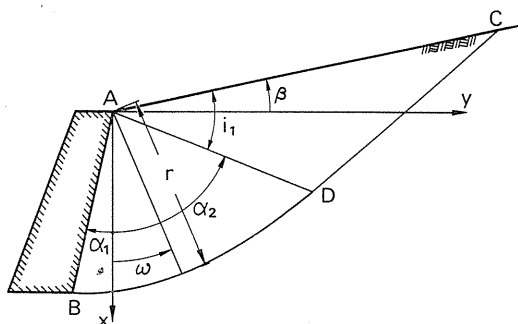


FIG. 11. Explanation of the Sokolovski method.

$$i_1 = \frac{1}{2}(\beta_0 - \Delta_0) + \frac{\pi}{4} - \frac{\phi}{2}. \quad (34)$$

Also referring Fig. 11, the angle  $\alpha_2$  between  $x$ -axis and sliding surface AD is given by the following equation;

$$2\alpha_2 = \phi + \frac{\pi}{2} + \beta + \theta_0 + \Delta_0. \quad (35)$$

### 3. Calculation of Passive Earth Pressure during Earthquake by the Sokolovski Method

Sokolovski<sup>8)</sup> has given the active and passive earth pressure of critical equilibrium in the static state assuming that the stress component  $\tilde{\sigma}$  was proportional to radius vector  $r$ . In order to calculate the passive earth pressure during earthquake with this method, we consider the plane critical equilibrium using the plane-polar coordinates  $(r, \omega)$  as shown in Fig. 12.

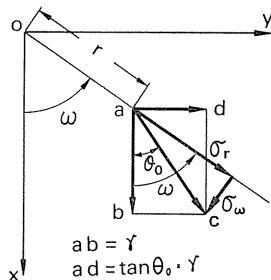


FIG. 12. Stresses in the soil mass during earthquake.

The differential equations of equilibrium are as follows;

$$\left. \begin{aligned} \frac{\partial \sigma_r}{\partial r} + \frac{1}{r} \frac{\partial \tau_{r\omega}}{\partial \omega} + \frac{\sigma_r - \sigma_\omega}{r} &= \gamma_0 \cos(\omega - \theta_0), \\ \frac{\partial \tau_{r\omega}}{\partial r} + \frac{1}{r} \frac{\partial \sigma_\omega}{\partial \omega} + \frac{2\tau_{r\omega}}{r} &= -\gamma_0 \sin(\omega - \theta_0). \end{aligned} \right\} \quad (36)$$

The above equations are in the case when the seismic force acts in the positive direction of  $y$ -axis as shown in Fig. 12.

The stress components  $\sigma_r$ ,  $\sigma_\omega$  and  $\tau_{r\omega}$  at critical plastic equilibrium are represented by the following equations;

$$\left. \begin{aligned} \sigma_r &= \bar{\sigma}(1 + \sin \phi \cos 2\phi), \\ \sigma_w &= \bar{\sigma}(1 - \sin \phi \cos 2\phi), \text{ and} \\ \tau_{rw} &= -\bar{\sigma} \sin \phi \sin 2\phi, \end{aligned} \right\} \quad (37)$$

where  $\phi$  is the angle between the major principal plane and  $r$ -plane, and it is positive in counterclockwise from major principal plane. The relation between the angles  $\phi_1$ ,  $\theta$  and  $\phi$  is as follows;

$$\phi = \theta + \omega = \phi_1 - \beta + \omega, \quad (38)$$

where  $\theta$  is the angle between the major principal plane and  $x$ -plane. Hence, we introduce the following functions according to Sokolovski;

$$\left. \begin{aligned} \phi &= \phi(\omega), \\ \bar{\sigma} &= \gamma_0 r S(\omega). \end{aligned} \right\} \quad (39)$$

Substituting Eq. 37 into Eq. 36, we obtain the following equations;

$$\left. \begin{aligned} \frac{dS}{d\omega} &= \frac{\sin[2\phi - (\omega - \theta_0)] - S \sin 2\phi}{\cos 2\phi - \sin \phi}, \\ \frac{d\phi}{d\omega} - 1 &= \frac{\cos(\omega - \theta_0) - \sin \phi \cos[2\phi - (\omega - \theta_0)] - S \cos^2 \phi}{-2S \sin \phi (\cos 2\phi - \sin \phi)}. \end{aligned} \right\} \quad (40)$$

The above equations are given  $S$  and  $\phi$  which vary along the curved sliding surface  $BD$  when the soil body is failed along the sliding surface  $BDC$  as shown in Fig. 11. The region  $\triangle ADC$  is the passive Rankine zone and is given already in section 2.4. Accordingly, the values of  $\theta$ ,  $\phi$ ,  $\omega$  and  $S$  along the sliding surface  $AD$  are defined by the following equations;

$$\left. \begin{aligned} \theta &= \frac{1}{2}(\beta_0 - \Delta_0) - \beta - \frac{\pi}{2}, \\ \phi &= -\left(\frac{\pi}{4} - \frac{\phi}{2}\right), \\ \omega &= \alpha_2 = \frac{1}{2}\left(\phi + \frac{\pi}{2} + \beta + \theta_0 + \Delta_0\right), \text{ and} \\ S &= \frac{\cos(\alpha_2 - \beta)}{\cos^2 \phi} (\cos \beta_0 + \sqrt{\sin^2 \phi - \sin^2 \beta_0}). \end{aligned} \right\} \quad (41)$$

Now, the angle  $\delta$  of wall friction with which the passive earth pressure acts on the back surface  $AB$  of the wall, is considered positive when it acts as shown in Fig. 1 and Fig. 2. Parameters  $\theta$ ,  $\phi$ ,  $S$  and  $\omega$  along the back surface  $AB$  of the wall are given as follows;

$$\left. \begin{aligned} \theta &= \frac{1}{2}(\delta + \Delta' - \pi) - \alpha_1, \\ \phi &= \frac{1}{2}(\delta + \Delta' - \pi), \\ S &= S_0, \text{ and} \\ \omega &= \alpha_1. \end{aligned} \right\} \quad (42)$$

where

$$\sin \Delta' = \frac{\sin \delta}{\sin \phi}.$$

The variables  $\omega$ ,  $\phi$  and  $S$  along the surface AD are known. Along the surface AB, two variables  $\omega$  and  $\phi$  are known, but  $S_0$  is unknown. Therefore, we assume the value of  $S_0$ , and compute the variables  $S$  and  $\phi$  along the surface AD with the recurrence formula of Eq. 43. In order to get  $S_0$ , the calculation must be repeated until the computed values become equal to those of Eq. 41 along the surface AD with various assumption of  $S_0$ .

$$\begin{aligned} S_{i+1} &= S_i + \frac{\sin(2\phi_i - \omega_i + \theta_0) - S_i \sin 2\phi_i}{\cos 2\phi_i - \sin \phi} \cdot \Delta\omega, \\ \phi_{i+1} &= \phi_i + \left[ \frac{\cos(\omega_i - \theta_0) - \sin \phi \cos(2\phi_i - \omega_i + \theta_0) - S_i \cos^2 \phi + 1}{-2S_i \sin \phi (\cos 2\phi_i - \sin \phi)} \right] \cdot \Delta\omega. \end{aligned} \quad (43)$$

Thus, the coefficient  $K_{PE}$  of the passive earth pressure during earthquake is obtained by the following equation;

$$K_{PE} = \frac{S_0 \cos \delta (\cos \delta + \sqrt{\sin^2 \phi - \sin^2 \delta})}{\cos \theta_0 \cos \alpha_1}. \quad (44)$$

Also, the equation of sliding surface is given as follows;

$$r = r_1 \exp \left[ - \int_{\alpha_1}^{\omega} \cot(\phi - \mu) d\omega \right]. \quad (45)$$

The term  $\mu$  is given by  $\left( \frac{\pi}{4} - \frac{\phi}{2} \right)$ . The solution of Eq. 45 is not a logarithmic spiral because  $\phi$  varies with  $\omega$ .

We know the next three conditions by comparing  $\theta$  of Eq. 41 with that of Eq. 42.

The sliding surface BD is convex, if

$$2\alpha_1 < \delta + \Delta' + \beta + \theta_0 + \Delta_0. \quad (46. a)$$

The sliding surface BD is straight, if

$$2\alpha_1 = \delta + \Delta' + \beta + \theta_0 + \Delta_0. \quad (46. b)$$

The sliding surface BD is concave, if

$$2\alpha_2 > 2\alpha_1 > \delta + \Delta' + \beta + \theta_0 + \Delta_0. \quad (46. c)$$

If  $\alpha_1 \geq \alpha_2$ , it is easy to obtain the earth pressure as the wall exists in the passive Rankine zone.

The Sokolovski method above mentioned can not be easily used for the case of Eq. 46. c, because the discontinuous line appears in the backfill. Hence, the authors show the method of calculation of the passive earth pressure during earthquake for this case with the Sokolovski method. The values of  $\phi$  and  $S$  on the discontinuous line AR in Fig. 13 are given by the following equations<sup>8)</sup>;

$$\tan \phi = \frac{1 - \sin \phi}{1 + \sin \phi} \cot \psi_{1-1}, \quad (47)$$

$$S = S_1 \frac{\sin 2\psi_{1-1}}{\sin 2\psi}. \quad (48)$$

The value of  $\psi_{1-1}$  is given by the next equation for the region I in Fig. 13;

$$\psi_{1-1} = \theta_1 + \alpha_3, \quad (49)$$

where  $\alpha_3$  is angle between  $x$ -axis and discontinuous line AR as shown in Fig.

13. The value of  $\theta_1$  is the angle between the  $x$ -axis and the major principal axis in the region I, and is shown in Eq. 41 as  $\theta$ . And also  $S_1$  is given by the next equation;

$$S_1 = \frac{\cos(\alpha_3 - \beta)}{\cos^2 \phi} (\cos \beta_0 + \sqrt{\sin^2 \phi - \sin^2 \beta_0}). \quad (50)$$

$\phi$  and  $S$  are obtained by Eq. 47 and Eq. 48, assuming the value of  $\alpha_3$ .

Using the values of  $\phi$  and  $S$  on the discontinuous line AR, we can calculate the values of  $\phi$  and  $S$  on the wall which is inclined  $\alpha_1$  to the vertical. In order to determine the value of  $S_n$  on the wall, the next recurrence formula are used until the calculated value of  $\phi_n$  on the wall becomes equal to the given  $\phi$ .

$$S_{i+1} = S_i - \frac{\sin(2\psi_i - \omega_i + \theta_0) - S_i \sin 2\psi_i}{\cos 2\psi_i - \sin \phi} \Delta\omega, \quad (51)$$

$$\psi_{i+1} = \psi_i - \left[ \frac{\cos(\omega_i - \theta_0) - \sin \phi \cos(2\psi_i - \omega_i + \theta_0) - S_i \cos^2 \phi}{-2S_i \sin \phi (\cos 2\psi_i - \sin \phi)} + 1 \right] \Delta\omega.$$

The value of  $\alpha'_1$  corresponding to  $\psi_n = \psi$  is obtained by the next equations;

$$\alpha'_1 = \alpha_3 - n\Delta\omega, \quad (52.a)$$

where

$$\Delta\omega = \frac{1}{3000} (\alpha_3 - \alpha_1). \quad (52.b)$$

The relationship between  $\alpha_3$  and  $\alpha'_1$  is shown in Fig. 14 as an example. Since the value of  $\alpha'_1$  must satisfy the next equation, the value of  $\alpha_3$  is determined as shown in Fig. 14.

$$\alpha'_1 = \alpha_1. \quad (53)$$

The values of  $K_{PE}$  obtained with this method are shown in Tables A-3, A-4 and A-5. However, the value of  $\Delta\omega$  in Eq. 52.b gives the very small error to the calculation of  $S$  on the wall. The sliding surface obtained by the solution of the discontinuous line corresponds to the concave curve obtained by the logarithmic spiral method as shown in these Tables. The value of  $K_{PE}$  obtained by the discontinuous line is smaller 3.0% at the maximum than that of the spiral method.

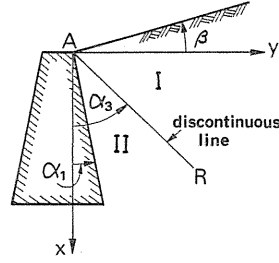


FIG. 13. Discontinuous line and angle of  $\alpha_3$ .

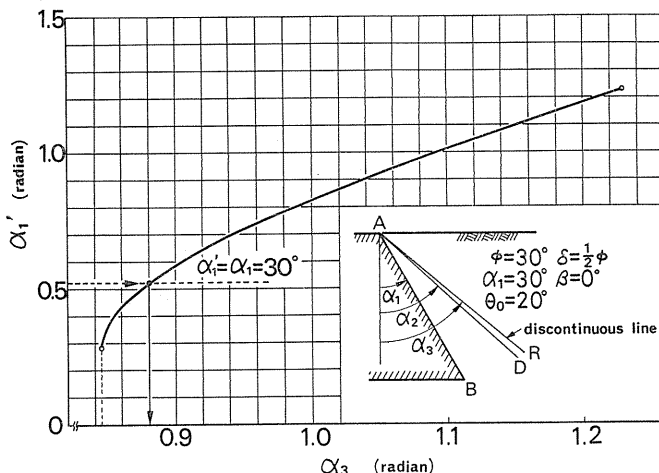


FIG. 14. Relationship between  $\alpha_1'$  and  $\alpha_3$ .

#### 4. Comparison of Results by the Logarithmic Spiral Method and by Other Methods

##### 4.1. Coefficient $K_{PE}$ of Passive Earth Pressure

The authors calculated the values of  $K_{PE}$  in the spiral method with a pitch of  $\Delta\omega=0.2^\circ$ . In the Sokolovski method, the variables of  $S$  and  $\phi$  along the surface  $AD$  which were obtained from the surface  $AB$  were calculated down to four places of decimals so as to agree with the values of  $S$  and  $\phi$  along the surface  $AD$  in Eq. 41. The value of  $\Delta\omega$  in the recurrence formula Eq. 43 is taken as  $\Delta\omega=(\alpha_2-\alpha_1)/1000$  in the case of  $\delta=1/2\cdot\phi$  and as  $\Delta\omega=(\alpha_2-\alpha_1)/3000$  in the case of  $\delta=2/3\cdot\phi$  and  $\delta=\phi$ . In this article, the authors give the coefficients of passive earth pressure during earthquake corresponding to the magnitude of the angle of the wall friction  $\delta$ .

##### (1) The case of $\delta=0^\circ$

The comparison of the values of  $K_{PE}$  which are obtained by the spiral method and the Mononobe method in the case of  $\delta=0^\circ$  and  $\alpha_1=\beta=0^\circ$  is shown in Fig. 15. The values of  $K_{PE}$  of the Mononobe method are nearly equal to those of the spiral method. In Fig. 16, the sliding surfaces which are obtained by the Sokolovski method and the spiral method are shown in this case. In Fig. 17, and Fig. 18, the values of  $K_{PE}$  which are obtained by the Mononobe method and the spiral method are shown for various value of  $\alpha_1$  and  $\beta$  in the case of  $\delta=0^\circ$ . The value of  $K_{PE}$  of the Mononobe method is greater than that of the spiral method as decreasing in the value of  $\alpha_1$ , or as

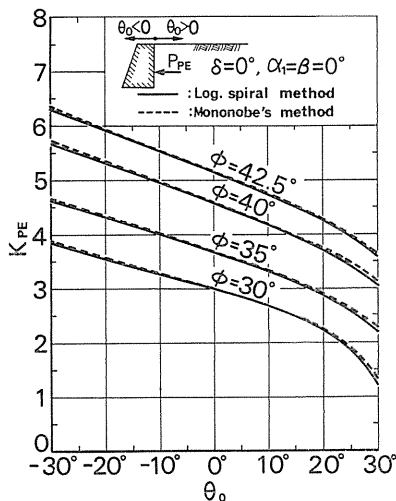


FIG. 15. Comparison between  $K_{PE}$  of the spiral method and that of the Mononobe method in the case of  $\alpha_1=\beta=0^\circ$  and  $\delta=0^\circ$ .



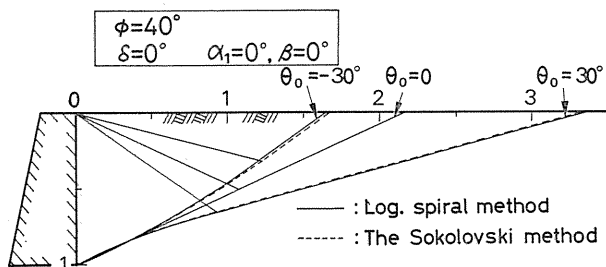


FIG. 16. Sliding surfaces obtained by the logarithmic spiral method and the Sokolovski method in the case of  $\alpha_1=\beta=0^\circ$  and  $\delta=0^\circ$ .

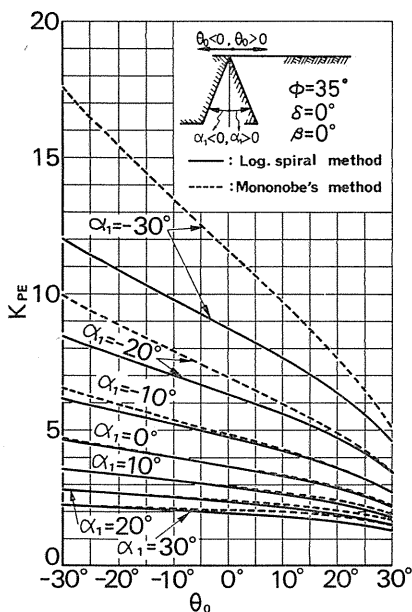


FIG. 17. Comparison between  $K_{PE}$  of the spiral method and that of the Mononobe method for various  $\alpha_1$  and  $\theta_0$  in the case of  $\delta=0^\circ$  and  $\beta=0^\circ$ .

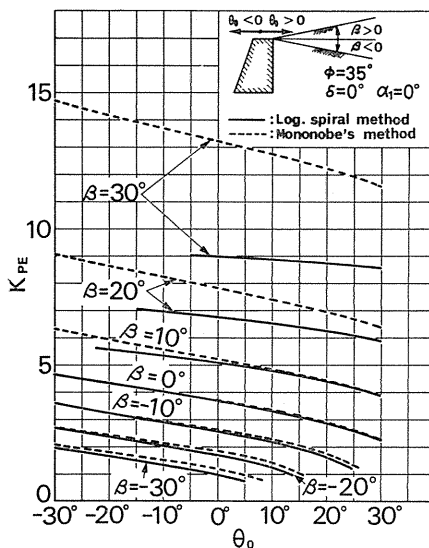


FIG. 18. Comparison between  $K_{PE}$  of the spiral method and that of the Mononobe method for various  $\beta$  and  $\theta_0$  in the case of  $\delta=0^\circ$  and  $\alpha_1=0^\circ$ .

increasing in the value of  $\beta$ . For example, in the case of  $\phi=35^\circ$ ,  $\alpha_1=-30^\circ$  and  $\theta_0=20^\circ$ , the value of  $K_{PE}$  of the Mononobe method is greater than that of the spiral method by 27%, and in the case of  $\phi=35^\circ$ ,  $\beta=30^\circ$  and  $\theta_0=20^\circ$ , the former is greater than the latter by 39%.

(2) The case of  $\delta=\pm 1/2 \cdot \phi$  and  $\delta=2/3 \cdot \phi$

In the case of  $\delta=1/2 \cdot \phi$  and  $\alpha_1=\beta=0^\circ$ , the values of  $K_{PE}$  and  $\omega_0$  are shown in Table A-1 for many values of  $\theta_0$  including  $\theta_0 < 0$ . The value of  $\omega_0$  is necessary to draw the sliding surface. The value of  $K_{PE}$  are graphically shown in Fig. 19. The values of  $K_{PE}$  of the spiral method coincide well with those of the Sokolovski method. In the case of  $\delta=2/3 \cdot \phi$  and  $\alpha_1=\beta=0^\circ$ , the values of  $K_{PE}$  are shown

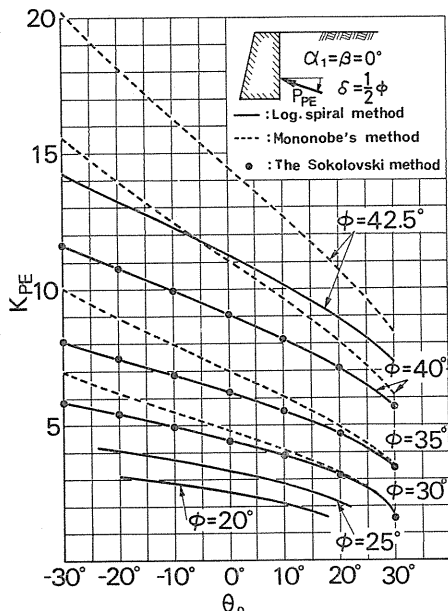


FIG. 19. Value of  $K_{PE}$  obtained by the spiral method, the Mononobe method and the Sokolovski method in the case of  $\delta=1/2\cdot\phi$  and  $\alpha_1=\beta=0^\circ$ .

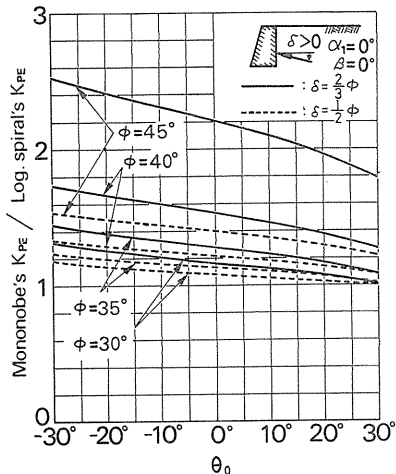


FIG. 20. Ratios of  $K_{PE}$  of the Mononobe method versus that of the spiral method in the case of  $\alpha_1=0^\circ$  and  $\beta=0^\circ$  under the conditions of  $\delta=1/2\cdot\phi$  and  $\delta=2/3\cdot\phi$ .

in Table A-2, for many values of  $\theta_0$  including  $\theta_0 < 0$ .

In Fig. 20, the ratio of  $K_{PE}$  of the Mononobe method to that of the spiral method are shown in the case of  $\delta=1/2\cdot\phi$  and  $\delta=2/3\cdot\phi$ . This figure represents that this ratio increases as the value of  $\delta$  increases. For an example, in the case of  $\delta=1/2\cdot\phi=20^\circ$  and  $\theta_0 \geq 20^\circ$ , the value of  $K_{PE}$  of the Mononobe method is greater 10% to 20% than that of the spiral method, and in the case of  $\delta=2/3\cdot\phi=26.7^\circ$  and  $\theta_0 \geq 0^\circ$ , the former is greater 30% to 50% than the latter. It is remarkable that the coefficients  $K_{PE}$  of the Mononobe method approach to those of the spiral method as the value of  $\theta_0$  increases. In Fig. 21, the ratios of  $K_{PE}$  of the spiral method in the case of  $\delta=1/2\cdot\phi$  and  $\delta=2/3\cdot\phi$  to that in the case of  $\delta=0^\circ$  are shown under the condition of  $\alpha_1=\beta=0^\circ$ . In the case of  $\delta=1/2\cdot\phi=20^\circ$  and  $\theta_0 \geq 0^\circ$ , the values of  $K_{PE}$  are 1.8 to 2.2 times of the values for  $\delta=0^\circ$ , and in the case of  $\delta=2/3\cdot\phi=26.7^\circ$ , the values of  $K_{PE}$  are 2.2 to 2.4 times of the values for  $\delta=0^\circ$ .

The calculation of the passive earth pressure in the case of  $\delta=1/2\cdot\phi$  and  $\delta=2/3\cdot\phi$  is very important for the design of retaining walls, because the practical angle of wall friction is almost considered as  $\delta \leq 2/3\cdot\phi$ . Hence, in Table A-3 and Table A-4, the values of  $K_{PE}$  of the spiral method and the Sokolovski method for  $\alpha_1$  or  $\beta$  is not zero and  $\theta_0 \geq 0^\circ$  are shown in the case of  $\delta=0^\circ$ ,  $\delta=1/2\cdot\phi$ ,  $\delta=2/3\cdot\phi$  and  $\phi=20^\circ \sim 45^\circ$ . In these Tables, the values of  $\omega_0$  in parentheses indicate the cases of the concave curves. Further, the values of  $K_{PE}$  and  $\omega_0$  in the case of  $\delta=1/2\cdot\phi=20^\circ$  and  $\beta=20^\circ$  are shown in Fig. 22 and Fig. 23 for various values of  $\alpha_1$  and  $\theta_0$ . In Fig. 22, the comparison of  $K_{PE}$  of the Sokolovski method to that

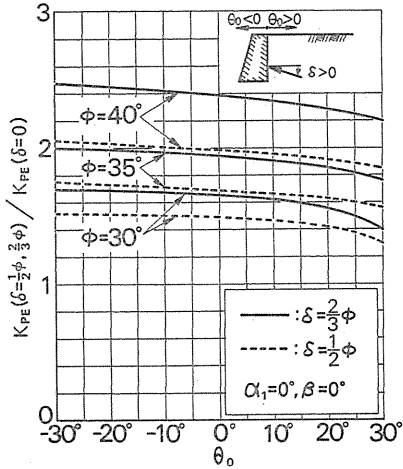


FIG. 21. Ratios of  $K_{PE}$  for  $\delta = 1/2 \cdot \phi$  or  $\delta = 2/3 \cdot \phi$  versus  $K_{PE}$  for  $\delta = 0^\circ$  by the spiral method.

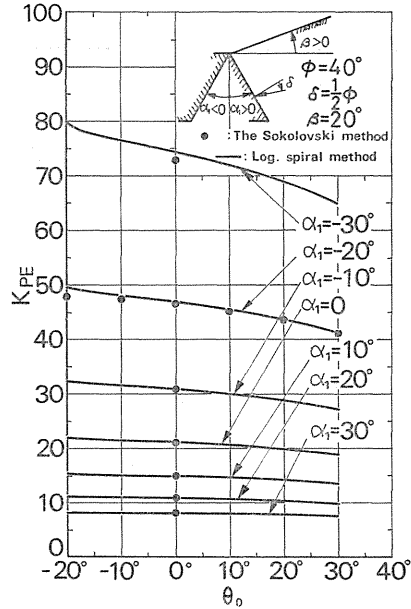


FIG. 22. Values of  $K_{PE}$  for various values of  $\alpha_1$  and  $\theta_0$  in the case of  $\beta = 20^\circ$  and  $\delta = 1/2 \cdot \phi = 20^\circ$ .

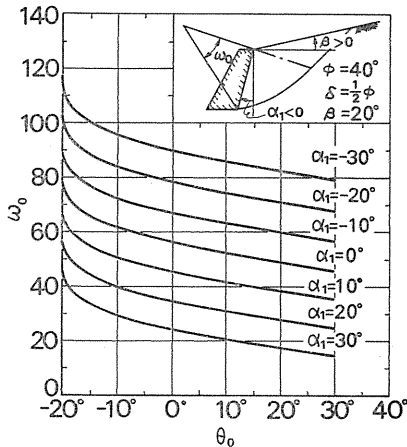


FIG. 23. Values of  $\omega_0$  for various values of  $\alpha_1$  and  $\theta_0$  in the case of  $\beta = 20^\circ$  and  $\delta = 1/2 \cdot \phi = 20^\circ$ .

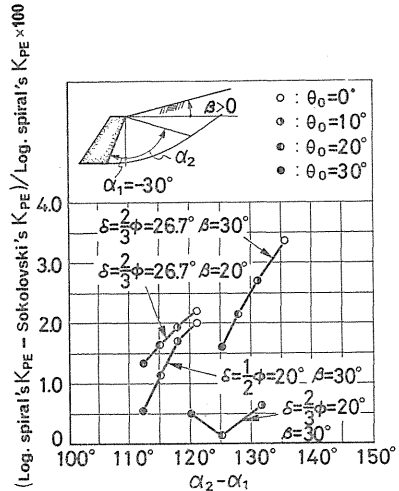


FIG. 24. Percent difference between  $K_{PE}$  of the spiral method and that of the Sokolovski method for various values of  $(\alpha_2 - \alpha_1)$  in the cases of  $\delta = 2/3 \cdot \phi$  and  $\delta = 1/2 \cdot \phi$ .

of the spiral method is shown.

The differences of  $K_{PE}$  of the spiral method and the Sokolovski method vary with  $(\alpha_2 - \alpha_1)$  and  $\delta$ . In Fig. 24, the percent difference of  $K_{PE}$  of the methods are shown for the cases of  $\delta = 2/3 \cdot \phi = 26.7^\circ$ ,  $\delta = 2/3 \cdot \phi = 20^\circ$  and  $\delta = 1/2 \cdot \phi = 20^\circ$  under the condition of  $\alpha_1 = -30^\circ$ ,  $\beta = 20^\circ$  and  $\theta_0 = 0^\circ \sim 30^\circ$ . In this figure, it is obtained

that the maximum percent difference of  $K_{PE}$  of the methods is 3.4% for the case of  $\alpha_1 \geq -30^\circ$ ,  $\beta \leq 30^\circ$ ,  $\delta \leq 2/3 \cdot \phi$  and  $(\alpha_2 - \alpha_1) \leq 136^\circ$ .

(3) The case of  $\delta = \phi$

In general, the passive earth pressure along the plane sliding surface of soil mass is calculated with the assumption of  $\delta = \phi$ . The values of  $K_{PE}$  and  $\omega_0$  of the spiral method are shown in Fig. 25 and Fig. 26 in the case of  $\delta = \phi = 30^\circ$  and  $\beta = 0^\circ$  for various values of  $\alpha_1$ . In Fig. 25, the values of  $K_{PE}$  by the Sokolovski method are also shown, comparing with  $K_{PE}$  of the spiral method. The ratios of  $K_{PE}$  of the spiral method to that of the Sokolovski method are shown in Fig. 27 in the case of  $\delta = \phi = 30^\circ$  and  $\beta = 0^\circ$ . From this figure, it can be understood that these ratios increase with decreasing in the value of  $\alpha_1$ . The value of  $K_{PE}$  of the spiral method is greater 21% than that of the Sokolovski method in the case of  $\theta_0 = 20^\circ$  and  $\alpha_1 = -70^\circ$ . And in the case of  $\theta_0 = 20^\circ$  and  $\alpha_1 = -50^\circ$ , the former is greater 6% than the latter. However, in the case of  $\alpha_1 \geq 0^\circ$ , the difference of the values of  $K_{PE}$  by the methods does not exceed 2.0%.

In Table A-6, the values of  $K_{PE}$  in the case of  $\delta = \phi$  are shown. The differ-

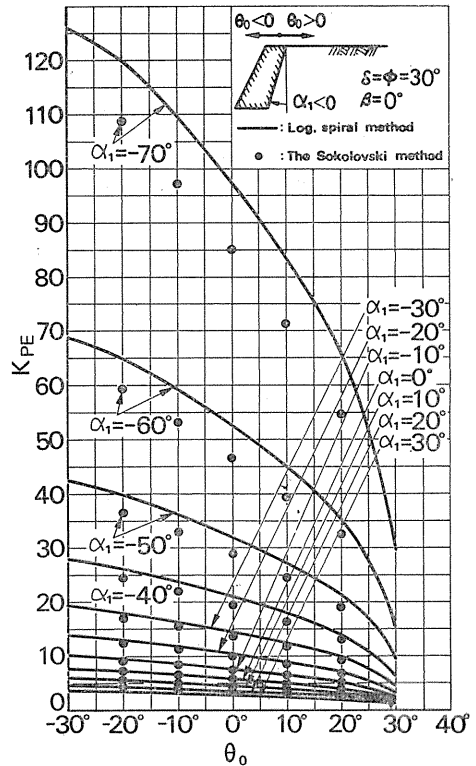


FIG. 25. Values of  $K_{PE}$  for various values of  $\alpha_1$  and  $\theta_0$  in the case of  $\delta = \phi = 30^\circ$  and  $\beta = 0^\circ$ .

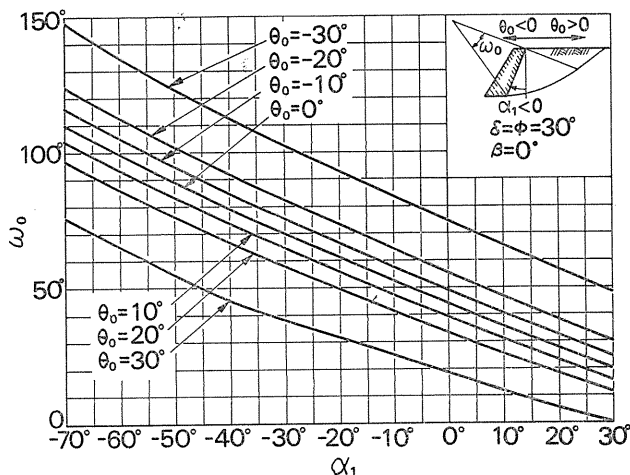


FIG. 26. Values of  $\omega_0$  for various values of  $\alpha_1$  and  $\theta_0$  in the case of  $\delta = \phi = 30^\circ$  and  $\beta = 0^\circ$ .

ence of these  $K_{PE}$  by the methods for the case of  $\delta = \phi$  is larger than that for the case of  $\delta = 1/2 \cdot \phi$  and  $\delta = 2/3 \cdot \phi$ . The spiral method does not satisfy the boundary conditions at the backface of wall. But, the difference of  $K_{PE}$  between the spiral method and the Sokolovski method for the case of  $\delta \leq 2/3 \cdot \phi$  is so small in practice that the passive earth pressure against retaining walls can be obtained by the spiral method with enough accuracy.

4.2. Sliding Surface

(1) Relationship between sliding surface, angle of wall friction and angle of internal friction

In Fig. 28, the sliding surfaces obtained by the spiral method are shown for various angles of wall friction  $\delta$  in the case of  $\alpha_1 = \beta = 0^\circ$ ,  $\phi = 40^\circ$  and  $\theta_0 = 0$ . In this figure, we can know that the sliding surface extends far away from the wall as increasing in the angle of wall friction. In Fig. 29, the sliding surfaces obtained by the spiral method are shown for various angles of internal friction  $\phi$  in the case of  $\alpha_1 = \beta = 0^\circ$  and  $\theta_0 = 0^\circ$ . The sliding surface extends far away from the wall and becomes longer as increasing in the angle of internal friction.

(2) Relationship between sliding surface and seismic force

In Fig. 30, the sliding surfaces of the spiral method, the Sokolovski method and the Mononobe method are shown in the case of  $\alpha_1 = \beta = 0^\circ$  and  $\delta = 1/2 \cdot \phi = 20^\circ$ . As increasing in the value of  $\theta_0$  which shows the intensity of seismic force, the ratio of the straight part to the curved part of the sliding surface becomes

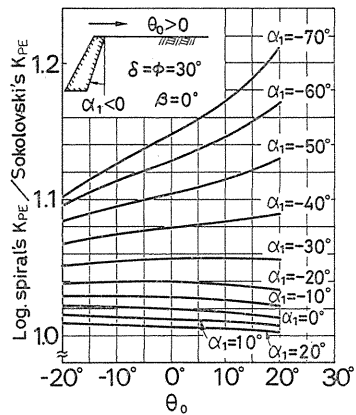


FIG. 27. Ratios of  $K_{PE}$  of the spiral method versus that of the Sokolovski method for various values of  $\alpha_1$  and  $\theta_0$  in the case of  $\delta = \phi = 30^\circ$  and  $\beta = 0^\circ$ .

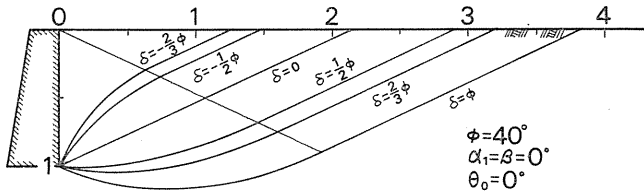


FIG. 28. Comparison of the sliding surfaces for various values of  $\delta$  in the case of  $\phi = 40^\circ$ ,  $\alpha_1 = \beta = 0^\circ$  and  $\theta_0 = 0^\circ$ .

larger and the sliding surface extends far away from the wall. The sliding surface of the Mononobe method approaches to that of the spiral method as the value of  $\theta_0$  increases. The sliding surfaces of the spiral method are almost the same with those of the Sokolovski method for  $\alpha_1 = 0^\circ$  and  $\beta = 0^\circ$ .

(3) Relationship between sliding surface and inclination of ground surface

In Fig. 31, the sliding surface obtained by the spiral method are shown for

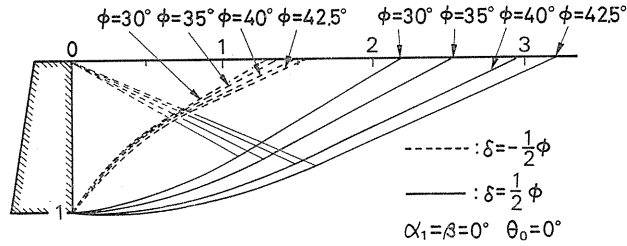


FIG. 29. Comparison of the sliding surfaces for various values of  $\phi$  in the case of  $\alpha_1=\beta=0^\circ$  and  $\theta_0=0^\circ$ .

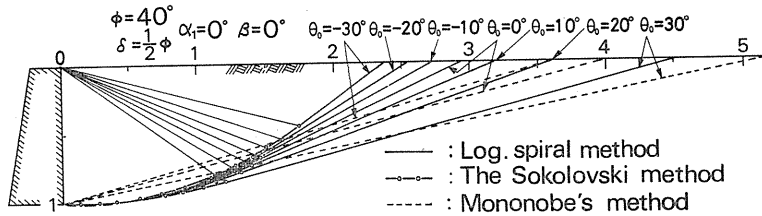


FIG. 30. Comparison of the sliding surfaces for various values of  $\theta_0$  in the case of  $\delta=1/2\cdot\phi=20^\circ$  and  $\alpha_1=\beta=0^\circ$ .

various inclination angle  $\beta$  of ground surface in the case of  $\phi=40^\circ$ ,  $\alpha_1=0^\circ$  and  $\theta_0=0^\circ$ . The ratio of the curved part to the straight part of sliding surface becomes larger as increasing in the value of  $\beta$ .

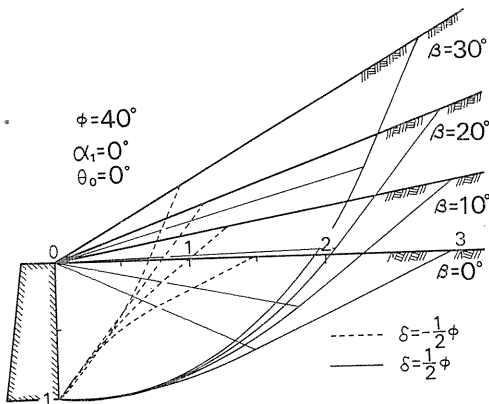


FIG. 31. Comparison of the sliding surfaces for various values of  $\beta$  in the case of  $\phi=40^\circ$ ,  $\alpha_1=0^\circ$  and  $\theta_0=0^\circ$ .

(4) Relationship between sliding surface and inclined angle of wall

In Fig. 32, the sliding surfaces obtained by the spiral method and the Sokolovski method are shown for  $\alpha_1=-30^\circ$ ,  $\alpha_1=0^\circ$  and  $\alpha_1=30^\circ$  in the case of  $\beta=20^\circ$ ,  $\delta=1/2\cdot\phi=20^\circ$  and  $\theta_0=0^\circ$ . The sliding surface becomes longer and the ratio of the curved part to the straight part of the sliding surface becomes larger as decreasing in the value of  $\alpha_1$ . Even in the case of  $\alpha_1=-30^\circ$ , the sliding surfaces of the spiral method do not practically differ from those of the Sokolovski method, and as shown before, the percent difference of  $K_{PE}$  of the

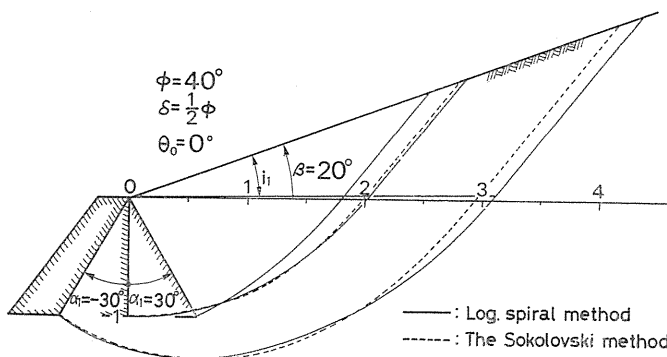


FIG. 32. Sliding surfaces for various values of  $\alpha_1$  in the case of  $\delta=1/2\cdot\phi=20^\circ$ ,  $\beta=20^\circ$  and  $\theta_0=0^\circ$ .

methods is 2.0% in the case of  $\alpha_1=-30^\circ$ .

(5) Comparison between sliding surface of the spiral method and that of Sokolovski method

In Fig. 33 the sliding surfaces obtained by the spiral method and the Sokolovski method in the case of  $\beta=0^\circ$ ,  $\alpha_1=-70^\circ$  and  $\delta=\phi=40^\circ$  are graphically shown. In this case, one sliding surface is the backface of the wall and the other sliding surface must intersect with backface of the wall at the angle of  $2\mu=\pi/2-\phi$ . The Sokolovski method satisfy this condition, but the spiral method does not satisfy this condition in Fig. 33.

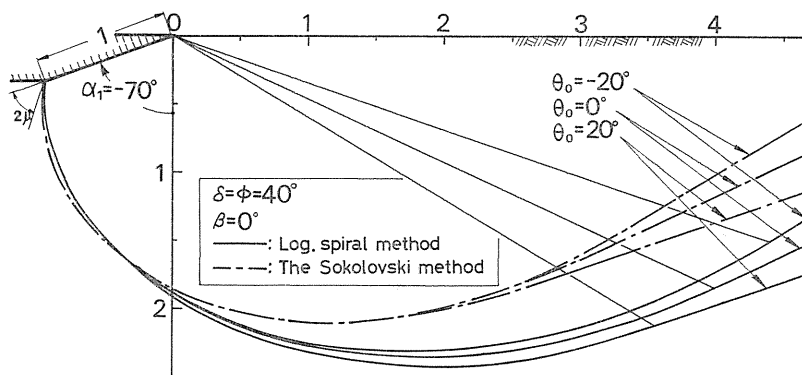


FIG. 33. Comparison between the sliding surface of the spiral method and that of the Sokolovski method in the case of  $\delta=\phi=40^\circ$ .

#### 4.3. Comparison between the Author's Results, Mayer-Vorfelder's Ones and Terzaghi's Ones

Mayer-Vorfelder (1970)<sup>2)</sup> obtained the horizontal coefficients of the passive earth pressure by means of the spiral method. The horizontal coefficient  $\lambda_{ph}$  by Mayer-Vorfelder can be converted to the coefficient  $K_p$  used in this paper with the following equation;

$$K_P = \frac{\cos \delta \cdot \cos \alpha_1}{\cos(\delta - \alpha_1)} \lambda p h. \tag{54}$$

The value of  $K_P$  for  $\delta = 1/2 \cdot \phi = 20^\circ$  by Mayer-Vorfelder are shown with the author's values in Fig. 34. In this case, Mayer-Vorfelder's results are coincide with the author's ones. But, in the case of  $\delta = \phi = 40^\circ$  and  $\alpha_1 = -30^\circ$ , the value of Mayer-Vorfelder is larger about 40% in comparison with the author's value as shown in Fig. 35.

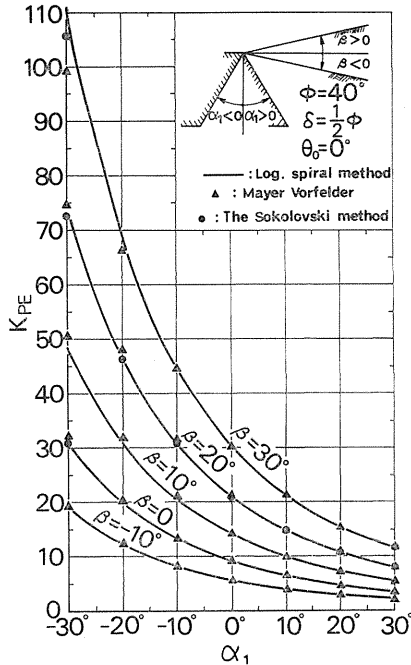


FIG. 34. Comparison between values of  $K_{PE}$  of the spiral method, those of Mayer-Vorfelder and those of the Sokolovski method in the case of  $\delta = 1/2 \cdot \phi = 20^\circ$ .

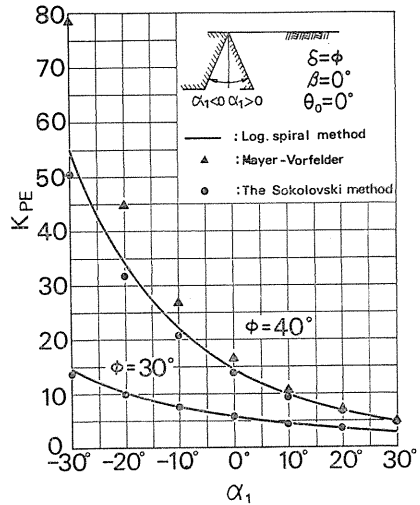


FIG. 35. Comparison between the values of  $K_{PE}$  of the spiral method, those of Mayer-Vorfelder and those of the Sokolovski method in the case of  $\delta = \phi$ .

Then, the authors compared their results by the spiral method with the values given by Terzaghi (1943)<sup>9)</sup> as shown in Fig. 36. The values of  $K_P$  according to Terzaghi in Fig. 36 were calculated with his values of  $N_\tau$  by the following equation;

$$K_P = \cos^2 \phi \left( \frac{2N_\tau}{\tan \phi} + 1 \right). \tag{55}$$

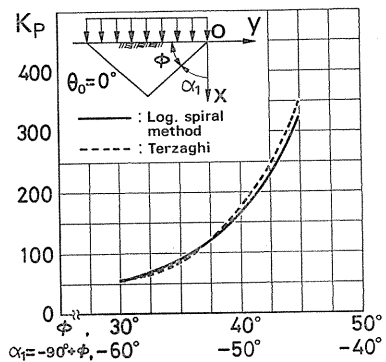


FIG. 36. Comparison between value of  $K_{PE}$  of the spiral method and that of  $N_\tau$  according to Terzaghi.

In the calculation of  $K_P$  with Eq. 55, the inclined angle of wall is given as  $\alpha_1 =$



$\phi=90^\circ$ . Fig. 36 shows a good agreement of Terzaghi's values with the author's ones. The difference of both results is 7% in the case of  $\delta=\phi=40^\circ$  and  $\alpha_1=-50^\circ$ . Mayer-Vorfelder's results are greater than those of the Sokolovski method and our logarithmic spiral method in the case of  $\delta=\phi=40^\circ$ , because his calculation is based on the "Gleichgewichts-Verfahren"<sup>2)</sup> suggested by him.

## 5. Conclusions

We compared the coefficients of the passive earth pressure obtained by the Sokolovski method, the logarithmic spiral method and the Mononobe method. Considering the rationality of the sliding surface, the Sokolovski method is best of all. Because, the Sokolovski method satisfies three conditions of equilibrium, *i.e.*  $\Sigma H=0$ ,  $\Sigma V=0$  and  $\Sigma M=0$ , in the sliding soil mass and boundary conditions of the Rankine region and of the wall. The spiral method satisfies only the condition of  $\Sigma M=0$  of the sliding soil mass and the boundary condition of the Rankine region. The Mononobe method satisfies conditions of  $\Sigma H=0$  and  $\Sigma V=0$  of the sliding soil mass, but does not satisfy boundary conditions of the Rankine region and of the wall.

The logarithmic spiral method is calculated more easily than the Sokolovski method, and the values of  $K_{PE}$  of the spiral method are almost same with those of the Sokolovski method in the case of  $\delta \leq 2/3 \cdot \phi$  and  $\alpha_1 \geq -30^\circ$ . Therefore, the values of  $K_{PE}$  for design of retaining wall can be calculated practically by the spiral method.

The results obtained by the authors are summarized as follows.

(1) Equation 46 gives the shape of sliding surface of the Sokolovski method. This equation is useful to distinguish between the convex sliding surface and concave sliding surface of the spiral method.

(2) The value of  $K_{PE}$  of the Mononobe method is reasonable only for the condition of  $\delta=0^\circ$  and  $\alpha_1=\beta=0^\circ$ . In the case of  $\delta=0^\circ$  and  $\alpha_1$  or  $\beta$  is not zero, the value of  $K_{PE}$  of the Mononobe method differs considerably from that of the spiral method. For an example, in the case of  $\phi=35^\circ$ ,  $\theta_0=20^\circ$ ,  $\alpha_1=-30^\circ$  and  $\beta=0^\circ$ , the former is greater 27% than the latter.

(3) As increasing in the value of  $\delta$  under the same conditions of  $\alpha_1$ ,  $\beta$ ,  $\phi$  and  $\theta_0$ , the value of  $K_{PE}$  of the Mononobe method becomes greater than that of the spiral method. For an instance, the former is greater 30% to 50% than the latter in the case of  $\delta=2/3 \cdot \phi=26.7^\circ$ ,  $\alpha_1=\beta=0^\circ$  and  $\theta_0=0^\circ$ .

(4) As increasing in the value of  $\theta_0$  under the condition of  $\alpha_1=\beta=0^\circ$  and  $\delta \approx 0^\circ$ , the values of  $K_{PE}$  of the Mononobe method and the spiral method approach gradually to that of the Sokolovski method.

(5) As increasing in the value of  $\delta$  and  $(\alpha_2-\alpha_1)$ , the value of  $K_{PE}$  of the spiral method becomes greater than that of the Sokolovski method. However, even in the case of  $\delta=2/3 \cdot \phi=26.7^\circ$ ,  $\alpha_1=-30^\circ$ ,  $\beta=30^\circ$  and  $(\alpha_2-\alpha_1)=135.5^\circ$ , the percent difference of  $K_{PE}$  of the methods is only 3.4%.

(6) In the case of  $\delta=\phi=30^\circ$ , the value of  $K_{PE}$  of the spiral method is greater about 6% than that of the Sokolovski method for the condition of  $\alpha_1=-30^\circ$ ,  $\beta=0^\circ$ ,  $\theta_0=20^\circ$  and  $(\alpha_2-\alpha_1)=78.4^\circ$ . Further, for the condition of  $\alpha_1=-70^\circ$ ,  $\beta=0^\circ$ ,  $\theta_0=20^\circ$  and  $(\alpha_2-\alpha_1)=118.4^\circ$ , the former is greater about 21% than the latter.

(7) In the case of  $\delta=\phi=40^\circ$ , the value of  $K_P$  of Mayer-Vorfelder is greater

40% than that of the spiral method under the condition of  $\alpha_1 = -30^\circ$ ,  $\beta = 0^\circ$  and  $\theta_0 = 0^\circ$ , and Terzaghi's value of  $K_p$  which is calculated from his value of  $N_T$  is greater 7% than that of the spiral method under the condition of  $\alpha_1 = -50^\circ$ ,  $\beta = 0^\circ$  and  $\theta_0 = 0^\circ$ .

(8) As increasing in the value of  $\theta_0$ , the sliding surface extends far away from the wall and becomes longer.

The authors wish to thank Professor K. Ueshita for his encouragement and co-operation. These calculations were made with FACOM 230-60 Computer at Nagoya University Computing Center.

### References

- 1) Brinch Hansen, J.: Earth Pressure Calculation, pp. 15~20, 1953.
- 2) Mayer-Vorfelder, H. J.: Ein Beitrag zur Berechnung des Erdwiderstandes unter Ansatz der Logarithmischen Spirale als Gleitflächenfunktion, Von der Universität Stuttgart zur Erlangung der Würde eines Doktor-Ingenieurs genehmigte Abhandlung, pp. 19-22, pp. 217-223, 1970.
- 3) Anzo, Z.: The Equation of Earth Pressure and Its Graphical Solution, Proceeding of Japan Society of Civil Engineers, Vol. 25, No. 5, pp. 485-491, 1939.
- 4) Kármán, Th.: Über Elastische Grenzzustände, Proc. 2nd, International Congresses on Applied Mechanics, pp. 23-32, Zürich, 1926.
- 5) Krey, H.: Erddruck, Erdwiderstand und Tragfähigkeit des Baugrundes, 1936.
- 6) Ohde, J.: Zur Theorie der Erddruckes unter besonderer Berücksichtigung der Erddruck Verteilung, Die Bautechnik, Vol. 16, pp. 150-159, pp. 176-180, pp. 241-245, pp. 331-335, pp. 480-487, pp.570-571, pp. 753-761, 1938.
- 7) Caquot, A. and Kerisel, J.: Tables de Butée, de Poussée et de Force Portante des Fondations, Gauthier-Villars, Paris 1949.
- 8) Sokolovski, V. V.: Statics of Soil Media, pp. 137-172, 1960.
- 9) Terzaghi, K.: Theoretical Soil Mechanics, pp. 124-125, 1943.

Appendix

Appendix 1. Mononobe Equation

The Mononobe equation assumes that the sliding surface is consisted of a straight line and is calculated by the following equations;

$$P_{PE} = \frac{1}{2}(1 - k_1)\gamma H^2 \frac{K_{PE}}{\sin \alpha \cos \delta},$$

$$K_{PE} = \frac{\sin^2(\alpha + \theta_0 - \phi) \cdot \cos \delta}{\cos \theta_0 \sin \alpha \cdot \sin(\alpha + \theta_0 + \delta) \left[ 1 - \sqrt{\frac{\sin(\phi + \delta) \cdot \sin(\phi + \beta - \theta_0)}{\sin(\alpha + \theta_0 + \delta) \cdot \sin(\alpha + \beta)}} \right]^2},$$

$$\theta_0 = \frac{k}{1 - k_1}, \tag{A-1}$$

where  $P_{PE}$  is the resultant force due to the passive earth pressure during earthquake,  $K_{PE}$  is the passive earth pressure coefficient during earthquake,  $k$  is the coefficient of horizontal earthquake intensity and  $k_1$  is the coefficient of vertical earthquake intensity, respectively. In this study,  $\theta_0$  is given by Eq. 27.

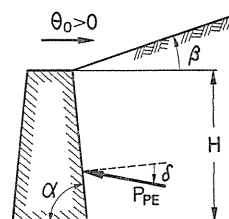


FIG. A-1. The Mononobe equation.

Appendix 2. Accuracy of Calculation

In the calculation of the Sokolovski method, there may be two kinds of errors. One is relating to the number of division of  $(\alpha_2 - \alpha_1)$ . The other is caused by the approximate solution in the case of  $\delta = \phi$ . The authors divided the value of  $(\alpha_2 - \alpha_1)$  into 1000 segments for the finite differential method in the case of  $\delta = 1/2 \cdot \phi$  and compared the results of the 1000-segment computation with those of the 4000-segment computation or the 6000-segment one. The values of  $K_{PE}$  computed for above 4000 or 6000 segment are almost the same regardless of the number of division. In Table A-7, the errors of the 1000-segment computations are shown. The values of  $K_{PE}$  become smaller as increasing in the number of division and decreasing in the value of  $(\alpha_2 - \alpha_1)$ . The maximum error of the 1000-segment computation is 0.6% in the case of  $\delta = 1/2 \cdot \phi$ . However, in the case of  $\delta = 2/3 \cdot \phi$  and  $\delta = \phi$ , we computed the value of  $K_{PE}$  not for 1000-segment but for 3000-segment. In Fig. A-2, the errors for various divisions are shown in the

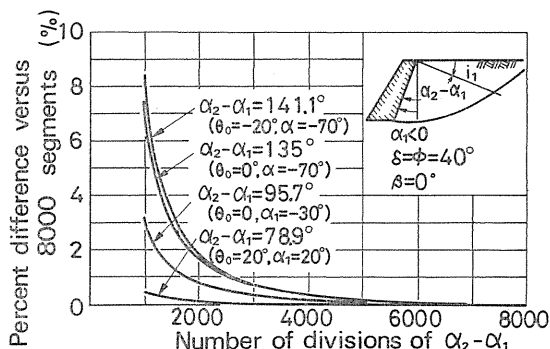


FIG. A-2. Percent difference of  $K_{PE}$  of the Sokolovski method computed with less division of  $(\alpha_2 - \alpha_1)$  versus that computed with 8000 division in the case of  $\delta = \phi = 40^\circ$ .

case of  $\delta = \phi = 40^\circ$ . As shown in this figure, the result of the 3000-segment computation is larger 0.78% than that of the 8000-segment one in the case of  $(\alpha_2 - \alpha_1) = 141.1^\circ$ .

In the case of  $\delta = \phi$ , the values of  $S$  and  $\phi$  at the backface of wall are discontinuous. Hence, in place of real backface of wall, the authors used the assumed backface which was inclined  $\Delta\omega'$  to the real backface according to Sokolovski.  $S'$ ,  $\phi'$  and  $\omega$  on the assumed backface of wall are given by the extended Sokolovski method using the following equations;

$$\left. \begin{aligned} (\phi' + \mu)^2 &= \frac{1}{2} \cot \phi \left[ 1 - \frac{\cos(\phi - \alpha_1 + \theta_0)}{S_0 \cos \phi} \right] (\omega - \alpha_1), \\ S' &= S_0 [1 + 2(\phi' + \mu) \tan \phi], \end{aligned} \right\} \quad (\text{A-2})$$

where  $\omega = \alpha_1 + \Delta\omega'$ .

The value of  $S_0$  on the real backface of wall is obtained by the method described relating to Eq. 43. In the case of  $\delta = \phi$ , the values of  $K_{PE}$  are calculated under the condition that  $\Delta\omega'$  equals to  $0.001^\circ$  and  $\alpha_2 - (\alpha_1 + \Delta\omega')$  is divided into 3000 segments. In Table A-8, the percent differences of  $K_{PE}$  of  $\Delta\omega' = 1^\circ$  and  $0.1^\circ$  versus that of  $\Delta\omega' = 0.001^\circ$  are presented. The error by a large value of  $\Delta\omega'$  seems to be compensated with the error of finite differential method. However, if we consider the shape of sliding surface near the wall, we must use the very small value of  $\Delta\omega'$ .

Next, we consider the errors of  $K_{PE}$  by the spiral method. The authors obtained the values of  $K_{PE}$  for various values of  $\Delta\omega$  and the percent differences of these values of  $K_{PE}$  from those of  $\Delta\omega = 0.01^\circ$  in Table A-9. From this Table, we can understand that the values of  $K_{PE}$  in the case of  $\Delta\omega = 0.2^\circ$  are satisfactory.

### Appendix 3. Passive Earth Pressure of Cohesive Soils and Passive Earth Pressure of Soils under Uniform Surcharge

If equation 46. a or 46. b is satisfied, we can use the foregoing results for medium possessing both internal friction and cohesion according to Sokolovski. In Fig. 1, assuming that the backfill possesses the uniform surcharge,  $q$  on the line AC and both internal friction and cohesion, the normal and tangential stresses on the wall are obtained by the next equations.

$$\left. \begin{aligned} \sigma_w &= \gamma x K_{PE} + p_{qE} \quad \text{and} \\ \tau_{wT} &= -(\gamma x K_{PE} + p_{qE} + c \cot \phi) \tan \delta, \end{aligned} \right\} \quad (\text{A-3})$$

where  $c$  is cohesion,  $\phi$  is the angle of internal friction of the backfill and  $\delta$  is the angle of wall friction.

$\gamma x K_{PE}$  is the normal pressure on the wall for an ideal granular medium ( $c=0$ ) possessing weight but without the surcharge on the boundary of the fill ( $q=0$ ). The values of  $K_{PE}$  are shown in Tables 1~6.  $p_{qE}$  is the normal pressure on the wall for a soil medium lacking weight ( $\gamma=0$ ).

In Fig. 1, the point of A is a singular point, and is replaced by a characteristic,  $\xi = \xi_0$ . Along this sliding surface,  $\tilde{\sigma}$  is given by the next formula.

$$\tilde{\sigma} = C e^{2 \psi_1 \tan \phi}, \quad (\text{A-4})$$

where  $C$  is constant,  $\phi_1$  is the angle between  $u$ -plane and major principal plane. The normal and tangential stresses on  $\overline{AC}$  are given by the following equations.

$$\left. \begin{aligned} \sigma_u &= q_E \cos \beta_0 \text{ and} \\ \tau_{uv} &= -q_E \sin \beta_0, \end{aligned} \right\} \quad (\text{A-5})$$

where  $q_E$  equals  $q/\cos \theta_0$ ,  $\beta_0$  and  $\theta_0$  are shown in Eqs. 26 and 27 respectively. Denoting the reduced load as  $q_1$  on  $\overline{AC}$  ( $v$ -axis) and the inclined angle to the normal line of  $\overline{AC}$  as  $\delta_1$ , the following equations can be obtained.

$$\left. \begin{aligned} \sigma_u + c \cot \phi &= q_E \cos \beta_0 + c \cot \phi = q_1 \cos \delta_1 \text{ and} \\ \tau_{uv} &= -q_E \sin \beta_0 = q_1 \sin \delta_1, \end{aligned} \right\} \quad (\text{A-6})$$

where

$$\tan \delta_1 = -\frac{q_E \sin \beta_0}{q_E \cos \beta_0 + c \cot \phi}. \quad (\text{A-7})$$

Also, we can obtain the next equations considering Mohr's circle.

$$\left. \begin{aligned} q_1 \cos \delta_1 &= \bar{\sigma} (1 + \sin \phi \cos 2\phi_1) \text{ and} \\ q_1 \sin \delta_1 &= -\bar{\sigma} \sin \phi \sin 2\phi_1. \end{aligned} \right\} \quad (\text{A-8})$$

Therefore,  $\phi_1$  and  $\bar{\sigma}$  are given by the following equations.

$$\left. \begin{aligned} 2\phi_1 &= -\delta_1 + A_1 - \pi, \\ \bar{\sigma} &= q_1 \frac{\sin A_1}{\sin (A_1 - \delta_1)}, \\ \sin A_1 &= \frac{\sin \delta_1}{\sin \phi} \text{ and} \\ \frac{\pi}{2} &\geq A_1 \geq -\frac{\pi}{2}. \end{aligned} \right\} \quad (\text{A-9})$$

The normal pressure  $p_{qE}$  on the backface of wall is given as follows, using the reduced stress  $p_1$ .

$$\left. \begin{aligned} \sigma_w + c \cot \phi &= p_{qE} + c \cot \phi = p_1 \cos \delta \text{ and} \\ \tau_{wr} &= -\tau_{rw} = -p_1 \sin \delta, \end{aligned} \right\} \quad (\text{A-10})$$

where

$$\left. \begin{aligned} p_1 \cos \delta &= \bar{\sigma} (1 - \sin \phi \cos 2\phi) \text{ and} \\ p_1 \sin \delta &= -\bar{\sigma} \sin \phi \sin 2\phi. \end{aligned} \right\} \quad (\text{A-11})$$

and  $\phi$  is the angle between the major principal plane and the backface of wall. In order to calculate the passive earth pressure against the wall the next relations can be derived.

$$\left. \begin{aligned} 2\psi &= \delta + \mathcal{A}' - \pi, \\ \tilde{\sigma} &= \frac{p_1 \sin \mathcal{A}'}{\sin(\delta + \mathcal{A}')} \quad \text{and} \\ \sin \mathcal{A}' &= \frac{\sin \delta}{\sin \phi}, \end{aligned} \right\} \quad (\text{A-12})$$

where  $\psi = \phi_1 + \alpha_1 - \beta$ .

Therefore, using the equations A-12, the value of  $\phi_1$  on the wall can be derived as follows.

$$2\phi_1 = \delta + \mathcal{A}' - \pi - 2\alpha_1 + 2\beta. \quad (\text{A-13})$$

Using the equations A-4, A-9, A-12, A-13, the next equation can be obtained.

$$\begin{aligned} p_1 &= q_1 \frac{(\cos \delta_1 + \sqrt{\cos^2 \delta_1 - \cos^2 \phi})(\cos \delta + \sqrt{\cos^2 \delta - \cos^2 \phi})}{1 - \sin^2 \phi} \\ &\quad \cdot \exp[(\delta + \mathcal{A}' + \delta_1 - \mathcal{A}_1 - 2\alpha_1 + 2\beta)\tan \phi]. \end{aligned} \quad (\text{A-14})$$

If  $\beta = 0^\circ$ ,  $\theta = 0^\circ$  and  $\delta_1 = 0^\circ$ , the values of  $\mathcal{A}_1$  equals zero and the following equation can be derived by equation A-14.

$$\begin{aligned} p_q + c \cot \phi &= (q + c \cot \phi) \frac{\cos \delta (\cos \delta + \sqrt{\cos^2 \delta - \cos^2 \phi})}{1 - \sin \phi} \\ &\quad \cdot \exp[(\delta + \mathcal{A}' - 2\alpha_1)\tan \phi]. \end{aligned} \quad (\text{A-15})$$

This equation is the same with that derived by Sokolovski. The value of  $p_1/q_1$  is obtained by equation A-14 and the value of  $p_{qE}$  can be determined by the following equation.

$$p_{qE} = \frac{p_1}{q_1} \left( \frac{\cos \delta}{\cos \delta_1} \right) (q_E \cos \beta_0 + c \cot \phi) - c \cot \phi. \quad (\text{A-16})$$

Thus,  $\sigma_w$  and  $\tau_{wr}$  against the wall can be obtained by equation A-3. If  $\tau_{wr}$  is negative, the tangential stress on the backface of wall acts upwards.

In Fig. A-3, the values of  $p_1/q_1$  are shown for various values of  $\phi$  in the case of  $\alpha_1 = \beta = 0^\circ$  and  $\delta = 1/2 \cdot \phi$ . In Fig. A-4, the values of  $p_{qE}$  are shown for specified cohesion in the case of  $\alpha_1 = \beta = 0^\circ$ ,  $\delta = 1/2 \cdot \phi = 15^\circ$  and  $q = 2t/m^2$ . The comparison between the results of equation A-3 and the more exact solution are shown in Fig. A-5 and Fig. A-6. This exact solution can be obtained by use of the finite difference method for  $(c, \phi)$  materials. In Fig. A-5, the values of  $\sigma_w$  are shown for various values of  $\alpha_1$  in the case of  $\beta = 0^\circ$ ,  $\theta_0 = 10^\circ$ ,  $\delta = 1/2 \cdot \phi = 10^\circ$ ,  $c = 1t/m^2$  and  $q = 1t/m^2$ . In Fig. A-6, the values of  $\sigma_w$  are shown for various values of  $\beta$  in the case of  $\alpha_1 = 0^\circ$ ,  $\theta_0 = 10^\circ$ ,  $\delta = 1/2 \cdot \phi = 10^\circ$ ,  $c = 1t/m^2$  and  $q = 0$ . The results of equation A-3 yield the exact values or values rather less than the exact values. However, in the case of  $|\beta_0| > \phi$ ,  $\sigma_w$  and  $\tau_{wr}$  must be calculated by not Eq. A-3 but the exact method.

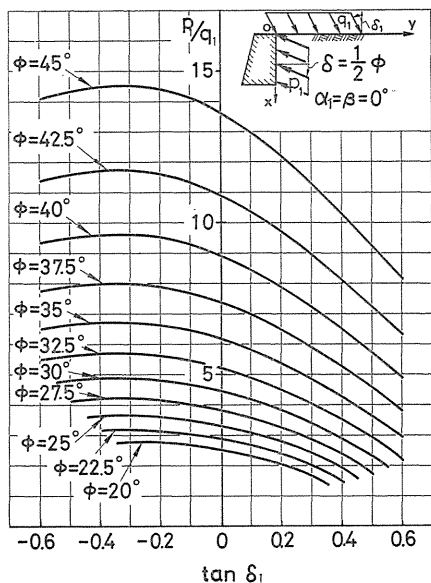


FIG. A-3. Values of  $p_1/q_1$  for various values of  $\phi$  in the case of  $\delta = 1/2 \cdot \phi$  and  $\alpha_1 = \beta = 0^\circ$ .

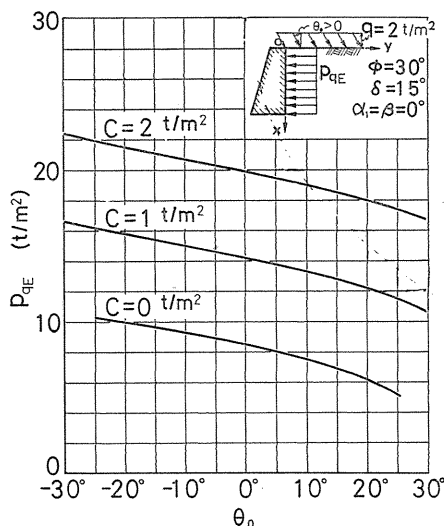


FIG. A-4. Values of  $p_{qE}$  for specified cohesion in the case of  $\alpha_1 = \beta = 0^\circ, \delta = 1/2 \cdot \phi = 15^\circ$  and  $q = 2 \text{ t/m}^2$ .

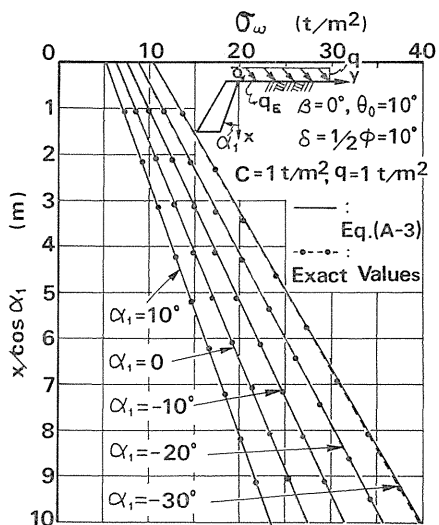


FIG. A-5. Comparison between values of  $\sigma_w$  of Eq. A-3 and those of the exact method in the case of  $\beta = 0^\circ, \theta_0 = 10^\circ, \delta = 1/2 \cdot \phi = 10^\circ, c = 1 \text{ t/m}^2$  and  $q = 1 \text{ t/m}^2$ .

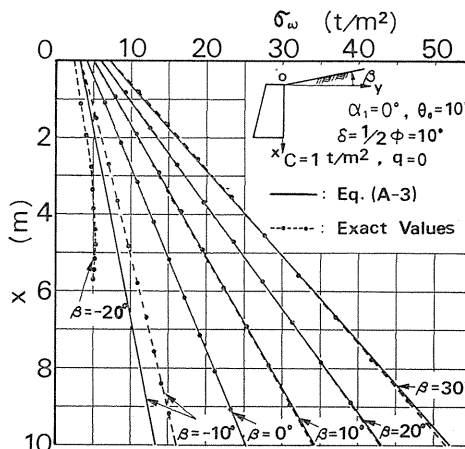


FIG. A-6. Comparison between values of  $\sigma_w$  of Eq. A-3 and those of the exact method in the case of  $\alpha_1 = 0^\circ, \theta_0 = 10^\circ, \delta = 1/2 \cdot \phi = 10^\circ, c = 1 \text{ t/m}^2$  and  $q = 0$ .







TABLE A-3 (2). Values of  $K_{PE}$  and  $\omega_0$  of the spiral method and the Sokolovski method for various values of  $\alpha_1$  in the case of  $\beta=0^\circ$ ,  $\delta=0^\circ$  and  $\phi=35^\circ \sim 45^\circ$ 

$\phi$	$\delta$	$\beta$	$\theta_0$	$K_{PE}$ $\omega_0$ (degrees)	$\alpha_1$	-30°	-20°	-10°	0°	10°	20°	30°
$\phi=35.0^\circ$	$\delta=0^\circ$	0°	Log. spiral method	$K_{PE}$	8.785	6.360	4.774	3.691	2.925	2.372	1.971	
			Sokolovski	$\omega_0$	34.3	22.7	11.3	(1.0)	(11.6)	(23.6)	(36.4)	
		10°	Log. spiral method	$K_{PE}$	7.696	5.626	4.265	3.329	2.664	2.183	1.835	
			Sokolovski	$\omega_0$	29.5	18.1	6.9	(4.0)	(15.8)	(27.8)	(40.8)	
	20°	Log. spiral method	$K_{PE}$	6.411	4.748	3.644	2.879	2.331	1.933	1.649		
		Sokolovski	$\omega_0$	23.8	12.8	1.8	(9.2)	(20.6)	(32.8)	(46.2)		
	30°	Log. spiral method	$K_{PE}$	4.613	3.494	2.733	2.205	1.819	1.538	1.349		
		Sokolovski	$\omega_0$	15.6	5.0	(5.6)	(16.6)	(28.2)	(41.0)	(53.7)		
	$\phi=37.5^\circ$	$\delta=0^\circ$	0°	Log. spiral method	$K_{PE}$	10.676	7.479	5.455	4.112	3.189	2.537	2.075
				Sokolovski	$\omega_0$	34.6	22.8	11.4	0.4	(11.5)	(23.5)	(36.1)
			10°	Log. spiral method	$K_{PE}$	9.427	6.664	4.906	3.733	2.923	2.349	1.942
				Sokolovski	$\omega_0$	30.3	18.9	7.5	(3.7)	(15.1)	(26.9)	(39.7)
20°		Log. spiral method	$K_{PE}$	7.977	5.706	4.250	3.271	2.590	2.106	1.764		
		Sokolovski	$\omega_0$	25.5	14.3	3.3	(7.9)	(19.1)	(31.1)	(44.1)		
30°		Log. spiral method	$K_{PE}$	6.045	4.407	3.343	2.618	2.108	1.742	1.490		
		Sokolovski	$\omega_0$	18.7	7.9	(2.9)	(13.7)	(24.9)	(37.1)	(50.7)		
$\phi=40.0^\circ$		$\delta=0^\circ$	0°	Log. spiral method	$K_{PE}$	13.115	8.865	6.268	4.600	3.484	2.718	2.185
				Sokolovski	$\omega_0$	34.8	23.0	11.4	(0.4)	(11.6)	(23.4)	(35.8)
			10°	Log. spiral method	$K_{PE}$	11.668	7.954	5.673	4.201	3.213	2.531	2.056
				Sokolovski	$\omega_0$	31.0	19.4	8.2	(3.0)	(14.6)	(26.4)	(38.8)
	20°	Log. spiral method	$K_{PE}$	10.010	6.897	4.973	3.724	2.879	2.293	1.885		
		Sokolovski	$\omega_0$	26.9	15.5	4.3	(6.5)	(18.0)	(29.6)	(42.2)		
	30°	Log. spiral method	$K_{PE}$	7.872	5.514	4.042	3.075	2.414	1.952	1.632		
		Sokolovski	$\omega_0$	21.5	10.3	(0.8)	(11.4)	(22.6)	(34.4)	(47.4)		
	$\phi=42.5^\circ$	$\delta=0^\circ$	0°	Log. spiral method	$K_{PE}$	16.316	10.605	7.247	5.260	3.817	2.915	2.302
				Sokolovski	$\omega_0$	35.1	23.1	11.5	(0.5)	(11.5)	(23.1)	(35.5)
			10°	Log. spiral method	$K_{PE}$	14.618	9.577	6.600	4.746	3.539	2.729	2.177
				Sokolovski	$\omega_0$	31.8	20.0	8.6	(2.7)	(14.1)	(25.7)	(37.9)
20°		Log. spiral method	$K_{PE}$	12.696	8.399	5.848	4.250	3.204	2.497	2.014		
		Sokolovski	$\omega_0$	28.2	16.6	5.2	(5.7)	(16.9)	(28.5)	(40.7)		
30°		Log. spiral method	$K_{PE}$	10.276	6.897	4.874	3.594	2.749	2.173	1.779		
		Sokolovski	$\omega_0$	23.6	12.2	1.2	(9.7)	(20.7)	(32.1)	(44.5)		
$\phi=45.0^\circ$		$\delta=0^\circ$	0°	Log. spiral method	$K_{PE}$	20.600	12.823	8.442	5.829	4.193	3.132	2.427
				Sokolovski	$\omega_0$	35.3	23.1	11.5	0.3	(11.4)	(23.0)	(35.2)
			10°	Log. spiral method	$K_{PE}$	18.582	11.652	7.733	5.385	3.909	2.947	2.307
				Sokolovski	$\omega_0$	32.4	20.6	9.0	(2.4)	(13.6)	(25.2)	(37.2)
	20°	Log. spiral method	$K_{PE}$	16.318	10.324	6.919	4.867	3.570	2.720	2.152		
		Sokolovski	$\omega_0$	29.4	17.6	6.2	(5.0)	(16.0)	(27.4)	(39.4)		
	30°	Log. spiral method	$K_{PE}$	13.521	8.665	5.885	4.198	3.122	2.410	1.932		
		Sokolovski	$\omega_0$	25.4	13.8	2.8	(8.2)	(19.0)	(30.4)	(42.4)		

TABLE A-3 (3). Values of  $K_{PE}$  and  $\omega_0$  of the spiral method and the Sokolovski method for various values of  $\alpha_1$  in the case of  $\beta=0^\circ$ ,  $\delta=1/2 \cdot \phi$  and  $20^\circ \sim 32.5^\circ$

$\phi$	$\delta$	$\beta$	$\theta_0$	$K_{PE}$ $\omega_0$ (degrees)	$\alpha_1$	-30°	-20°	-10°	0°	10°	20°	30°
						$K_{PE}$ $\omega_0$	$K_{PE}$ $\omega_0$	$K_{PE}$ $\omega_0$	$K_{PE}$ $\omega_0$	$K_{PE}$ $\omega_0$	$K_{PE}$ $\omega_0$	$K_{PE}$ $\omega_0$
$\phi=20.0^\circ$	$\delta=1/2 \cdot \phi$	$\beta=0^\circ$	0°	Log. spiral method	$K_{PE}$	4.179	3.467	2.934	2.520	2.191	1.921	1.698
				Sokolovski	$K_{PE}$	49.4	39.8	30.4	20.6	10.8	0.6	(11.4)
			10°	Log. spiral method	$K_{PE}$	3.388	2.846	2.436	2.114	1.854	1.639	1.462
				Sokolovski	$K_{PE}$	38.3	29.1	19.7	10.1	(0.6)	(11.4)	(25.6)
20°	Log. spiral method	$K_{PE}$	1.755	1.528	1.345	1.194	1.050	-----	-----			
	Sokolovski	$K_{PE}$	14.0	5.0	(5.0)	(17.0)	(28.0)	-----	-----			
30°	Log. spiral method	$K_{PE}$	-----	-----	-----	-----	-----	-----	-----			
	Sokolovski	$K_{PE}$	-----	-----	-----	-----	-----	-----	-----			
$\phi=22.5^\circ$	$\delta=1/2 \cdot \phi$	$\beta=0^\circ$	0°	Log. spiral method	$K_{PE}$	5.132	4.147	3.426	2.879	2.452	2.110	1.852
				Sokolovski	$K_{PE}$	50.7	40.9	31.3	21.5	11.5	1.1	(10.5)
			10°	Log. spiral method	$K_{PE}$	4.229	3.455	2.885	2.446	2.100	1.822	1.595
				Sokolovski	$K_{PE}$	41.2	31.8	22.4	12.8	2.6	(8.5)	(21.7)
20°	Log. spiral method	$K_{PE}$	2.886	2.407	2.046	1.762	1.533	1.347	1.214			
	Sokolovski	$K_{PE}$	27.4	18.4	9.2	0.4	(12.1)	(26.1)	(44.7)			
30°	Log. spiral method	$K_{PE}$	-----	-----	-----	-----	-----	-----	-----			
	Sokolovski	$K_{PE}$	-----	-----	-----	-----	-----	-----	-----			
$\phi=25.0^\circ$	$\delta=1/2 \cdot \phi$	$\beta=0^\circ$	0°	Log. spiral method	$K_{PE}$	6.364	5.001	4.029	3.308	2.757	2.327	1.984
				Sokolovski	$K_{PE}$	51.9	41.9	32.1	22.3	12.3	1.7	(9.6)
			10°	Log. spiral method	$K_{PE}$	5.318	4.219	3.429	2.840	2.387	2.029	1.743
				Sokolovski	$K_{PE}$	43.8	34.2	24.6	14.8	4.8	(6.0)	(18.6)
20°	Log. spiral method	$K_{PE}$	3.892	3.139	2.590	2.173	1.847	1.587	1.385			
	Sokolovski	$K_{PE}$	33.1	23.9	14.5	4.7	(5.8)	(18.0)	(33.8)			
30°	Log. spiral method	$K_{PE}$	-----	-----	-----	-----	-----	-----	-----			
	Sokolovski	$K_{PE}$	-----	-----	-----	-----	-----	-----	-----			
$\phi=27.5^\circ$	$\delta=1/2 \cdot \phi$	$\beta=0^\circ$	0°	Log. spiral method	$K_{PE}$	7.976	6.089	4.775	3.825	3.118	2.577	2.155
				Sokolovski	$K_{PE}$	53.2	45.0	33.0	23.2	13.2	2.6	(8.7)
			10°	Log. spiral method	$K_{PE}$	6.749	5.194	4.106	3.316	2.723	2.267	1.909
				Sokolovski	$K_{PE}$	46.1	36.3	26.5	16.7	6.7	(4.1)	(16.1)
20°	Log. spiral method	$K_{PE}$	5.160	4.024	3.221	2.632	2.184	1.836	1.564			
	Sokolovski	$K_{PE}$	37.5	27.9	18.3	8.7	(1.7)	(13.1)	(27.1)			
30°	Log. spiral method	$K_{PE}$	-----	-----	-----	-----	-----	-----	-----			
	Sokolovski	$K_{PE}$	-----	-----	-----	-----	-----	-----	-----			
$\phi=30.0^\circ$	$\delta=1/2 \cdot \phi$	$\beta=0^\circ$	0°	Log. spiral method	$K_{PE}$	10.122	7.493	5.712	4.458	3.547	2.867	2.350
				Sokolovski	$K_{PE}$	54.4	44.0	34.0	24.0	13.8	3.4	(8.0)
			10°	Log. spiral method	$K_{PE}$	8.662	6.456	4.957	3.896	3.122	2.542	2.098
				Sokolovski	$K_{PE}$	48.4	38.2	28.4	18.4	8.4	(2.2)	(14.0)
20°	Log. spiral method	$K_{PE}$	6.837	5.151	3.997	3.175	2.569	2.110	1.758			
	Sokolovski	$K_{PE}$	41.0	31.2	21.4	11.8	1.6	(9.4)	(22.4)			
30°	Log. spiral method	$K_{PE}$	3.025	2.375	1.912	1.567	1.304	1.107	1.000			
	Sokolovski	$K_{PE}$	21.6	12.4	3.0	(7.2)	(19.4)	(35.2)	(59.0)			
$\phi=32.5^\circ$	$\delta=1/2 \cdot \phi$	$\beta=0^\circ$	0°	Log. spiral method	$K_{PE}$	13.031	9.336	6.904	5.239	4.063	3.208	2.573
				Sokolovski	$K_{PE}$	55.7	45.3	35.1	24.9	14.7	4.1	(7.1)
			10°	Log. spiral method	$K_{PE}$	11.269	8.120	6.042	4.616	3.604	2.864	2.313
				Sokolovski	$K_{PE}$	50.4	40.2	30.0	20.0	9.8	(0.3)	(12.1)
20°	Log. spiral method	$K_{PE}$	9.121	6.629	4.978	3.838	3.024	2.424	1.975			
	Sokolovski	$K_{PE}$	44.3	34.3	24.3	14.3	4.3	(6.5)	(18.7)			
30°	Log. spiral method	$K_{PE}$	5.839	4.330	3.317	2.605	2.087	1.700	1.413			
	Sokolovski	$K_{PE}$	33.6	24.0	14.4	4.6	(5.7)	(17.7)	(32.5)			

TABLE A-3 (4). Values of  $K_{PE}$  and  $\omega_0$  of the spiral method and the Sokolovski method for various values of  $\alpha_1$  in the case of  $\beta=0^\circ$ ,  $\delta=1/2\cdot\phi$  and  $\phi=35^\circ\sim 45^\circ$ 

$\phi$	$\delta$	$\beta$	$\theta_0$	$K_{PE}$		$\alpha_1$	-30°	-20°	-10°	0°	10°	20°	30°
				$\omega_0$ (degrees)									
$\phi=35.0^\circ$	$\delta=1/2\cdot\phi$	$\beta=0^\circ$	0°	Log. spiral method	$K_{PE}$	$\alpha_1$	17.056	11.800	8.446	6.220	4.692	3.612	2.831
				Sokolovski method	$\omega_0$		56.9	46.3	36.1	25.7	15.5	4.9	(6.2)
				Log. spiral method	$K_{PE}$		14.895	10.353	7.451	5.520	4.190	3.247	2.561
				Sokolovski method	$\omega_0$		52.5	42.1	31.7	21.5	11.3	0.9	(10.6)
			20°	Log. spiral method	$K_{PE}$	12.311	8.616	6.249	4.667	3.572	2.791	2.220	
				Sokolovski method	$\omega_0$	47.2	36.8	26.8	16.8	6.6	(4.0)	(15.8)	
				Log. spiral method	$K_{PE}$	8.667	6.152	4.528	4.666	2.664	2.109	1.702	
				Sokolovski method	$\omega_0$	39.2	29.2	19.2	9.4	(0.6)	(11.8)	(25.0)	
			30°	Log. spiral method	$K_{PE}$	22.756	15.162	10.479	7.469	5.468	4.096	3.132	
				Sokolovski method	$\omega_0$	58.4	47.6	37.2	26.8	16.4	5.8	(5.3)	
				Log. spiral method	$K_{PE}$	20.055	13.414	9.313	6.674	4.914	3.704	2.851	
				Sokolovski method	$\omega_0$	54.5	43.9	33.3	23.1	12.7	2.3	(8.9)	
20°	Log. spiral method	$K_{PE}$	16.876	11.349	7.930	5.724	4.247	3.226	2.502				
	Sokolovski method	$\omega_0$	49.9	39.5	29.1	18.9	8.7	(1.9)	(13.3)				
	Log. spiral method	$K_{PE}$	12.598	8.559	6.049	4.420	3.320	2.552	2.003				
	Sokolovski method	$\omega_0$	43.5	33.1	22.9	12.9	2.7	(7.9)	(20.1)				
30°	Log. spiral method	$K_{PE}$	31.044	19.863	13.213	9.089	6.440	4.683	3.485				
	Sokolovski method	$\omega_0$	59.8	48.8	38.2	27.6	17.2	6.6	(4.4)				
	Log. spiral method	$K_{PE}$	27.598	17.711	11.827	8.174	5.823	4.260	3.191				
	Sokolovski method	$\omega_0$	56.4	45.6	35.0	24.4	14.0	3.6	(7.6)				
20°	Log. spiral method	$K_{PE}$	23.592	15.205	10.205	7.099	5.092	3.753	2.832				
	Sokolovski method	$\omega_0$	52.5	41.7	31.1	20.9	10.5	0.3	(11.2)				
	Log. spiral method	$K_{PE}$	18.367	11.925	8.077	5.675	4.115	3.065	2.339				
	Sokolovski method	$\omega_0$	47.1	36.5	26.3	16.1	5.9	(4.8)	(16.4)				
30°	Log. spiral method	$K_{PE}$	43.466	26.613	16.979	11.234	7.678	5.405	3.906				
	Sokolovski method	$\omega_0$	61.3	50.1	39.3	28.7	18.1	7.5	(3.5)				
	Log. spiral method	$K_{PE}$	38.959	23.909	15.303	10.166	6.983	4.943	3.595				
	Sokolovski method	$\omega_0$	58.2	47.2	36.4	25.8	15.4	4.8	(6.3)				
20°	Log. spiral method	$K_{PE}$	33.777	20.795	13.366	8.927	6.171	4.399	3.223				
	Sokolovski method	$\omega_0$	54.8	44.0	33.2	22.6	12.2	1.8	(9.3)				
	Log. spiral method	$K_{PE}$	27.169	16.816	10.884	7.330	5.115	3.683	2.726				
	Sokolovski method	$\omega_0$	50.6	39.6	29.0	18.6	8.4	(2.1)	(13.3)				
30°	Log. spiral method	$K_{PE}$	62.747	36.613	22.312	14.139	9.288	6.306	4.413				
	Sokolovski method	$\omega_0$	62.7	51.5	40.5	29.7	19.1	8.3	(2.6)				
	Log. spiral method	$K_{PE}$	56.683	33.134	20.243	12.873	8.494	5.798	4.083				
	Sokolovski method	$\omega_0$	60.0	49.0	38.0	27.2	16.6	6.0	(5.0)				
20°	Log. spiral method	$K_{PE}$	49.772	29.162	17.876	11.419	7.577	5.206	3.693				
	Sokolovski method	$\omega_0$	57.2	46.0	35.2	24.6	14.0	3.4	(7.6)				
	Log. spiral method	$K_{PE}$	41.113	24.178	14.899	9.584	6.412	4.447	3.184				
	Sokolovski method	$\omega_0$	53.6	42.4	31.6	21.2	10.6	(0.4)	(10.8)				
30°	Log. spiral method	$K_{PE}$	31.044	19.863	13.213	9.089	6.440	4.683	3.485				
	Sokolovski method	$\omega_0$	59.8	48.8	38.2	27.6	17.2	6.6	(4.4)				
	Log. spiral method	$K_{PE}$	27.598	17.711	11.827	8.174	5.823	4.260	3.191				
	Sokolovski method	$\omega_0$	56.4	45.6	35.0	24.4	14.0	3.6	(7.6)				

TABLE A-3 (5). Values of  $K_{PE}$  and  $\omega_0$  of the spiral method and the Sokolovski method for various values of  $\alpha_1$  in the case of  $\beta=0^\circ$ ,  $\delta=2/3\cdot\phi$  and  $\phi=20^\circ \sim 32.5^\circ$

$\phi$	$\delta$	$\beta$	$\theta_0$	$K_{PE}$ $\omega_0$ (degrees)	$\alpha_1$	-30°	-20°	-10°	0°	10°	20°	30°
20°	2/3·phi	0°	0°	Log. spiral } $K_{PE}$	}	4.491	3.701	3.113	2.660	2.300	2.007	1.764
				Sokolovski } $K_{PE}$		54.2	45.0	35.8	26.8	17.6	8.2	(2.5)
			10°	Log. spiral } $K_{PE}$	}	3.631	3.028	2.575	2.221	1.937	1.705	1.506
				Sokolovski } $K_{PE}$		45.3	34.5	25.7	17.0	7.5	0.3	(15.1)
20°	0°	Log. spiral } $K_{PE}$	}	1.854	1.602	1.401	1.236	1.098	-----	-----		
		Sokolovski } $K_{PE}$		19.8	11.6	2.8	(8.0)	(22.2)	-----	-----		
30°	0°	Log. spiral } $K_{PE}$	}	-----	-----	-----	-----	-----	-----	-----		
		Sokolovski } $K_{PE}$		-----	-----	-----	-----	-----	-----	-----		
22.5°	2/3·phi	0°	0°	Log. spiral } $K_{PE}$	}	5.588	4.482	3.677	3.070	2.598	2.223	1.919
				Sokolovski } $K_{PE}$		55.7	46.3	37.1	27.9	18.7	9.1	0.5
			10°	Log. spiral } $K_{PE}$	}	4.595	3.723	3.085	2.597	2.215	1.909	1.658
				Sokolovski } $K_{PE}$		46.4	37.4	28.4	19.6	10.2	(0.4)	(11.4)
20°	0°	Log. spiral } $K_{PE}$	}	3.115	2.574	2.169	1.855	1.602	1.395	1.232		
		Sokolovski } $K_{PE}$		33.0	24.6	16.0	7.0	(3.1)	(15.5)	(33.3)		
30°	0°	Log. spiral } $K_{PE}$	}	-----	-----	-----	-----	-----	-----	-----		
		Sokolovski } $K_{PE}$		-----	-----	-----	-----	-----	-----	-----		
25°	2/3·phi	0°	0°	Log. spiral } $K_{PE}$	}	7.029	5.479	4.379	3.568	2.953	2.475	2.094
				Sokolovski } $K_{PE}$		57.1	47.5	38.1	28.9	19.5	9.9	(0.8)
			10°	Log. spiral } $K_{PE}$	}	5.865	4.610	3.715	3.051	2.544	2.147	1.828
				Sokolovski } $K_{PE}$		49.4	40.0	30.8	21.8	12.6	2.8	(8.4)
20°	0°	Log. spiral } $K_{PE}$	}	4.274	3.411	2.787	2.318	1.954	1.664	1.431		
		Sokolovski } $K_{PE}$		38.9	30.1	21.3	12.5	2.7	(8.2)	(22.4)		
30°	0°	Log. spiral } $K_{PE}$	}	-----	-----	-----	-----	-----	-----	-----		
		Sokolovski } $K_{PE}$		-----	-----	-----	-----	-----	-----	-----		
27.5°	2/3·phi	0°	0°	Log. spiral } $K_{PE}$	}	8.950	6.771	5.263	4.180	3.379	2.770	2.297
				Sokolovski } $K_{PE}$		58.6	49.0	39.4	30.0	20.6	11.0	1.0
			10°	Log. spiral } $K_{PE}$	}	7.566	5.764	4.513	3.610	2.938	2.424	2.022
				Sokolovski } $K_{PE}$		51.9	42.3	33.1	23.9	14.5	4.7	(6.1)
20°	0°	Log. spiral } $K_{PE}$	}	5.768	4.446	3.521	2.848	2.341	1.948	1.658		
		Sokolovski } $K_{PE}$		43.5	34.3	25.3	16.1	6.7	(3.5)	(15.9)		
30°	0°	Log. spiral } $K_{PE}$	}	-----	-----	-----	-----	-----	-----	-----		
		Sokolovski } $K_{PE}$		-----	-----	-----	-----	-----	-----	-----		
30°	2/3·phi	0°	0°	Log. spiral } $K_{PE}$	}	11.558	8.474	6.396	4.943	3.895	3.120	2.531
				Sokolovski } $K_{PE}$		60.2	50.2	40.6	31.0	21.6	11.8	1.8
			10°	Log. spiral } $K_{PE}$	}	9.888	7.290	5.537	4.307	3.416	2.752	2.246
				Sokolovski } $K_{PE}$		54.4	44.6	35.2	25.8	16.2	6.6	(3.8)
20°	0°	Log. spiral } $K_{PE}$	}	7.790	5.797	4.445	3.490	2.793	2.269	1.865		
		Sokolovski } $K_{PE}$		47.4	37.8	28.6	19.2	10.0	0.4	(11.4)		
30°	0°	Log. spiral } $K_{PE}$	}	3.396	2.625	2.085	1.688	1.385	1.152	1.000		
		Sokolovski } $K_{PE}$		28.4	19.6	10.8	1.6	(9.2)	(23.6)	(59.0)		
32.5°	2/3·phi	0°	0°	Log. spiral } $K_{PE}$	}	15.168	10.757	7.870	5.908	4.531	3.539	2.806
				Sokolovski } $K_{PE}$		61.7	51.7	41.9	32.5	22.7	12.9	2.7
			10°	Log. spiral } $K_{PE}$	}	13.120	9.346	6.873	5.188	4.003	3.145	2.507
				Sokolovski } $K_{PE}$		56.8	46.8	37.2	27.6	18.0	8.4	(2.1)
20°	0°	Log. spiral } $K_{PE}$	}	10.610	7.612	5.642	4.294	3.340	2.644	2.123		
		Sokolovski } $K_{PE}$		50.9	41.1	31.5	22.1	12.7	2.9	(8.1)		
30°	0°	Log. spiral } $K_{PE}$	}	6.760	4.935	3.723	2.883	2.277	1.827	1.487		
		Sokolovski } $K_{PE}$		40.4	31.2	22.0	12.8	3.2	(7.3)	(20.7)		

TABLE A-3 (6). Values of  $K_{PE}$  and  $\omega_0$  of the spiral method and the Sokolovski method for various values of  $\alpha_1$  in the case of  $\beta=0^\circ$ ,  $\delta=2/3\cdot\phi$  and  $\phi=35^\circ\sim 45^\circ$ 

$\phi$	$\delta$	$\beta$	$\theta_0$	KPE $\omega_0$ (degrees)	$\alpha_1$	-30°	-20°	-10°	0°	10°	20°	30°
$\phi=35.0^\circ$	$\delta=2/3\cdot\phi$	$\beta=0^\circ$	0°	Log. spiral } KPE method $\omega_0$ Sokolovski KPE		20.281 63.3	13.883 53.1	9.823 43.3	7.147 33.5	5.324 23.7	4.047 13.9	3.130 3.7
			10°	Log. spiral } KPE method $\omega_0$ Sokolovski KPE		17.722 59.1	12.174 48.9	8.651 39.1	6.324 29.3	4.737 19.7	3.621 9.9	2.815 (0.6)
			20°	Log. spiral } KPE method $\omega_0$ Sokolovski KPE		14.647 54.0	10.116 44.0	7.234 34.2	5.325 24.6	4.017 15.2	3.093 5.4	2.421 (5.2) 2.421
			30°	Log. spiral } KPE method $\omega_0$ Sokolovski KPE		10.290 46.2	7.189 36.4	5.206 27.0	3.883 17.6	2.967 8.2	2.311 (1.8)	1.829 (13.6) 1.828
$\phi=37.5^\circ$	$\delta=2/3\cdot\phi$	$\beta=0^\circ$	0°	Log. spiral } KPE method $\omega_0$ Sokolovski KPE		27.705 65.0	18.263 54.8	12.467 44.6	8.768 34.8	6.329 24.8	4.672 15.0	3.518 4.8
			10°	Log. spiral } KPE method $\omega_0$ Sokolovski KPE		24.442 61.3	16.155 51.1	11.066 41.1	7.815 31.1	5.668 21.3	4.207 11.5	3.184 1.3
			20°	Log. spiral } KPE method $\omega_0$ Sokolovski KPE		20.581 56.9	13.657 46.9	9.401 36.9	6.679 27.1	4.875 17.5	3.642 7.7	2.774 (2.9)
			30°	Log. spiral } KPE method $\omega_0$ Sokolovski KPE		15.357 50.7	10.270 40.7	7.136 30.9	5.122 21.3	3.779 11.7	2.853 1.9	2.194 (8.9) 2.193
$\phi=40.0^\circ$	$\delta=2/3\cdot\phi$	$\beta=0^\circ$	0°	Log. spiral } KPE method $\omega_0$ Sokolovski KPE		38.803 66.6	24.564 56.2	16.130 46.0	10.935 36.0 10.922	7.626 26.0	5.453 16.0	3.987 5.8
			10°	Log. spiral } KPE method $\omega_0$ Sokolovski KPE		34.543 63.4	21.910 53.0	14.427 42.8	9.814 32.8 9.814	6.873 23.0	4.939 13.0	3.629 2.8
			20°	Log. spiral } KPE method $\omega_0$ Sokolovski KPE		29.564 59.7	18.806 49.3	12.430 39.3	8.497 29.3 8.486	5.984 19.5	4.327 9.7	3.199 (1.0)
			30°	Log. spiral } KPE method $\omega_0$ Sokolovski KPE		23.034 54.7	14.729 44.5	9.802 34.5	6.755 24.7 6.750	4.801 14.9	3.503 5.1	2.614 (5.4) 2.614
$\phi=42.5^\circ$	$\delta=2/3\cdot\phi$	$\beta=0^\circ$	0°	Log. spiral } KPE method $\omega_0$ Sokolovski KPE		55.950 68.5	33.908 23.8	21.348 47.5	13.903 37.3	9.336 27.1	6.446 17.1	4.564 6.9
			10°	Log. spiral } KPE method $\omega_0$ Sokolovski KPE		50.234 65.6	30.485 55.0	19.232 44.6	12.561 34.6	8.466 24.4	5.871 14.4	4.177 4.2
			20°	Log. spiral } KPE method $\omega_0$ Sokolovski KPE		43.622 62.4	26.524 51.8	16.781 41.6	11.003 31.4	7.452 21.4	5.197 11.6	3.719 1.4
			30°	Log. spiral } KPE method $\omega_0$ Sokolovski KPE		35.144 58.2	21.442 47.8	13.632 37.6	8.995 27.6	6.138 17.6	4.316 7.8	3.115 (2.5)
$\phi=45.0^\circ$	$\delta=2/3\cdot\phi$	$\beta=0^\circ$	0°	Log. spiral } KPE method $\omega_0$ Sokolovski KPE		83.474 70.1	48.253 59.5	29.014 48.9	18.080 38.5	11.645 28.3	7.734 18.3	5.284 7.9
			10°	Log. spiral } KPE method $\omega_0$ Sokolovski KPE		75.553 67.6	43.711 57.0	26.323 46.6	16.440 36.2	10.622 26.0	7.083 16.0	4.862 5.8
			20°	Log. spiral } KPE method $\omega_0$ Sokolovski KPE		66.471 65.0	38.505 54.2	23.235 43.8	14.555 33.6	9.443 23.4	6.328 13.4	4.368 3.2
			30°	Log. spiral } KPE method $\omega_0$ Sokolovski KPE		55.026 61.4	31.942 50.8	19.340 40.4	12.174 30.2	7.947 20.2	5.365 10.2	3.733 (0.4)

TABLE A-4 (1). Values of  $K_{PE}$  and  $\omega_0$  of the spiral method and the Sokolovski method for various values of  $\beta$  in the case of  $\alpha_1=0^\circ$ ,  $\delta=0^\circ$  and  $\phi=20^\circ \sim 32.5^\circ$  (The values of  $\omega_0$  in parentheses indicate the case of the concave curve)

$\phi$	$\delta$	$\alpha_1$	$\theta_0$	$K_{PE}$ $\omega_0$ (degrees)	$\beta$	-30°	-20°	-10°	0°	10°	20°	30°
20.0°	0°	Log. spiral method	Sokolovski	K <sub>PE</sub> $\omega_0$	K <sub>PE</sub> K <sub>PE</sub>	-----	-----	1.516 (24.0)	2.040 (0.8)	2.530 25.3	-----	-----
						-----	-----	1.513	-----	-----	-----	
	10°	Log. spiral method	Sokolovski	K <sub>PE</sub> $\omega_0$	K <sub>PE</sub> K <sub>PE</sub>	-----	-----	0.931 (59.6)	1.744 (11.6)	2.322 11.2	2.867 34.5	3.482 79.2
						-----	-----	-----	1.744	-----	-----	-----
20°	Log. spiral method	Sokolovski	K <sub>PE</sub> $\omega_0$	K <sub>PE</sub> K <sub>PE</sub>	-----	-----	-----	1.052 (45.0)	2.019 0.5	2.672 22.2	3.307 45.7	
					-----	-----	-----	1.041	-----	-----	-----	
30°	Log. spiral method	Sokolovski	K <sub>PE</sub> $\omega_0$	K <sub>PE</sub> K <sub>PE</sub>	-----	-----	-----	-----	-----	2.354 10.7	3.133 33.0	
					-----	-----	-----	-----	-----	-----	-----	
22.5°	0°	Log. spiral method	Sokolovski	K <sub>PE</sub> $\omega_0$	K <sub>PE</sub> K <sub>PE</sub>	-----	1.056 (53.7)	1.656 (21.7)	2.240 (0.9)	2.820 21.3	3.414 49.3	-----
						-----	-----	1.653	-----	-----	-----	-----
	10°	Log. spiral method	Sokolovski	K <sub>PE</sub> $\omega_0$	K <sub>PE</sub> K <sub>PE</sub>	-----	-----	1.221 (38.3)	1.938 (9.7)	2.598 11.3	3.257 32.5	3.961 61.1
						-----	-----	1.211	1.938	-----	-----	-----
20°	Log. spiral method	Sokolovski	K <sub>PE</sub> $\omega_0$	K <sub>PE</sub> K <sub>PE</sub>	-----	-----	-----	1.447 (24.7)	2.288 1.6	3.050 22.5	3.838 43.7	
					-----	-----	-----	1.445	-----	-----	-----	
30°	Log. spiral method	Sokolovski	K <sub>PE</sub> $\omega_0$	K <sub>PE</sub> K <sub>PE</sub>	-----	-----	-----	-----	1.747 (12.7)	2.728 12.8	3.657 33.5	
					-----	-----	-----	-----	1.747	-----	-----	
25.0°	0°	Log. spiral method	Sokolovski	K <sub>PE</sub> $\omega_0$	K <sub>PE</sub> K <sub>PE</sub>	-----	1.182 (46.0)	1.808 (19.8)	2.464 (0.8)	3.151 19.6	3.879 43.5	-----
						-----	-----	1.805	-----	-----	-----	-----
	10°	Log. spiral method	Sokolovski	K <sub>PE</sub> $\omega_0$	K <sub>PE</sub> K <sub>PE</sub>	-----	-----	1.403 (31.8)	2.154 (8.0)	2.913 11.3	3.713 31.0	4.597 55.3
						-----	-----	1.397	2.154	-----	-----	-----
20°	Log. spiral method	Sokolovski	K <sub>PE</sub> $\omega_0$	K <sub>PE</sub> K <sub>PE</sub>	-----	-----	-----	1.699 (19.2)	2.594 3.2	3.493 22.5	4.473 42.4	
					-----	-----	-----	1.698	-----	-----	-----	
30°	Log. spiral method	Sokolovski	K <sub>PE</sub> $\omega_0$	K <sub>PE</sub> K <sub>PE</sub>	-----	-----	-----	-----	2.096 (7.6)	3.164 14.2	4.287 33.5	
					-----	-----	-----	-----	2.096	-----	-----	
27.5°	0°	Log. spiral method	Sokolovski	K <sub>PE</sub> $\omega_0$	K <sub>PE</sub> K <sub>PE</sub>	-----	1.306 (41.1)	1.974 (18.5)	2.710 (0.7)	3.529 18.4	4.427 39.8	-----
						-----	-----	1.289	1.972	-----	-----	-----
	10°	Log. spiral method	Sokolovski	K <sub>PE</sub> $\omega_0$	K <sub>PE</sub> K <sub>PE</sub>	-----	-----	1.582 (27.5)	2.396 (6.9)	3.276 11.4	4.248 29.8	5.366 51.6
						-----	-----	1.577	2.396	-----	-----	-----
20°	Log. spiral method	Sokolovski	K <sub>PE</sub> $\omega_0$	K <sub>PE</sub> K <sub>PE</sub>	-----	-----	-----	1.954 (15.5)	2.945 4.5	4.015 22.6	5.240 41.4	
					-----	-----	-----	1.953	-----	-----	-----	
30°	Log. spiral method	Sokolovski	K <sub>PE</sub> $\omega_0$	K <sub>PE</sub> K <sub>PE</sub>	-----	-----	-----	-----	2.464 (4.3)	3.678 15.5	5.051 33.8	
					-----	-----	-----	-----	2.464	-----	-----	
30.0°	0°	Log. spiral method	Sokolovski	K <sub>PE</sub> $\omega_0$	K <sub>PE</sub> K <sub>PE</sub>	-----	1.432 (37.6)	2.157 (17.4)	3.001 (0.6)	3.965 17.6	5.073 37.2	-----
						-----	-----	1.418	2.155	-----	-----	-----
	10°	Log. spiral method	Sokolovski	K <sub>PE</sub> $\omega_0$	K <sub>PE</sub> K <sub>PE</sub>	-----	-----	1.769 (24.6)	2.668 (5.8)	3.695 11.4	4.882 29.0	6.301 49.0
						-----	-----	1.765	2.668	-----	-----	-----
20°	Log. spiral method	Sokolovski	K <sub>PE</sub> $\omega_0$	K <sub>PE</sub> K <sub>PE</sub>	-----	-----	0.960 (47.8)	2.229 (12.8)	3.351 5.4	4.637 22.6	6.175 40.6	
					-----	-----	0.941	2.229	-----	-----	-----	
30°	Log. spiral method	Sokolovski	K <sub>PE</sub> $\omega_0$	K <sub>PE</sub> K <sub>PE</sub>	-----	-----	-----	1.202 (33.6)	2.875 (1.8)	4.289 16.4	5.987 34.0	
					-----	-----	-----	1.197	-----	-----	-----	
32.5°	0°	Log. spiral method	Sokolovski	K <sub>PE</sub> $\omega_0$	K <sub>PE</sub> K <sub>PE</sub>	-----	1.565 (34.9)	2.359 (16.5)	3.323 (0.7)	4.471 16.7	5.844 35.0	7.597 59.9
						-----	-----	1.553	2.357	-----	-----	-----
	10°	Log. spiral method	Sokolovski	K <sub>PE</sub> $\omega_0$	K <sub>PE</sub> K <sub>PE</sub>	-----	1.095 (46.9)	1.971 (22.5)	2.976 (4.9)	4.184 11.5	5.640 28.3	7.449 46.8
						-----	-----	1.967	2.976	-----	-----	-----
20°	Log. spiral method	Sokolovski	K <sub>PE</sub> $\omega_0$	K <sub>PE</sub> K <sub>PE</sub>	-----	-----	1.387 (33.1)	2.535 (10.9)	3.825 6.2	5.382 22.7	7.327 39.9	
					-----	-----	1.380	2.534	-----	-----	-----	
30°	Log. spiral method	Sokolovski	K <sub>PE</sub> $\omega_0$	K <sub>PE</sub> K <sub>PE</sub>	-----	-----	-----	1.807 (20.9)	3.323 0.7	5.024 17.4	7.144 34.3	
					-----	-----	-----	1.806	-----	-----	-----	

TABLE A-4 (2). Values of  $K_{PE}$  and  $\omega_0$  of the spiral method and the Sokolovski method for various values of  $\beta$  in the case of  $\alpha_1=0^\circ$ ,  $\delta=0^\circ$ , and  $\phi=35^\circ \sim 45^\circ$

$\phi$	$\delta$	$\beta$	$\theta_0$	$K_{PE}$ $\omega_0$ (degrees)	$\beta$	-30°	-20°	-10°	0°	10°	20°	30°
$\phi=35.0^\circ$	$\delta=0^\circ$	$\alpha_1=0^\circ$	0°	Log. spiral } $K_{PE}$ ----- method $\omega_0$ (32.8) Sokolovski } $K_{PE}$ 1.695		-----	1.707 (32.8)	2.584 (15.8)	3.691 (1.0)	5.064 15.9	6.770 33.2	8.995 54.8
			10°	Log. spiral } $K_{PE}$ ----- method $\omega_0$ (41.0) Sokolovski } $K_{PE}$ 1.255		-----	1.271 (41.0)	2.191 (20.6)	3.329 (4.0)	4.757 11.3	6.554 27.5	8.877 45.2
	20°	Log. spiral } $K_{PE}$ ----- method $\omega_0$ ----- Sokolovski } $K_{PE}$ -----		-----	1.651 (28.2)	2.879 (9.2)	4.381 6.9	6.284 22.9	8.764 39.3			
		30°	Log. spiral } $K_{PE}$ ----- method $\omega_0$ ----- Sokolovski } $K_{PE}$ -----		-----	2.205 (16.6)	3.870 2.0	5.914 18.3	8.593 34.3			
$\phi=37.5^\circ$	$\delta=0^\circ$	$\alpha_1=0^\circ$	0°	Log. spiral } $K_{PE}$ 1.117 method $\omega_0$ (50.9) Sokolovski } $K_{PE}$ 1.848		1.860 (31.1)	2.835 (15.1)	4.112 0.4	5.762 15.4	7.896 31.8	10.769 51.6	
			10°	Log. spiral } $K_{PE}$ ----- method $\omega_0$ (37.1) Sokolovski } $K_{PE}$ 1.427		-----	1.440 (37.1)	2.434 (19.1)	3.733 (3.7)	5.436 11.4	7.669 27.0	10.677 44.0
	20°	Log. spiral } $K_{PE}$ ----- method $\omega_0$ ----- Sokolovski } $K_{PE}$ -----		-----	1.913 (24.9)	3.271 (7.9)	5.041 7.7	7.387 23.0	10.582 38.8			
		30°	Log. spiral } $K_{PE}$ ----- method $\omega_0$ ----- Sokolovski } $K_{PE}$ -----		-----	2.618 (13.7)	4.515 3.3	7.007 18.9	10.432 34.6			
$\phi=40.0^\circ$	$\delta=0^\circ$	$\alpha_1=0^\circ$	0°	Log. spiral } $K_{PE}$ 1.224 method $\omega_0$ (47.4) Sokolovski } $K_{PE}$ 2.013		2.205 (29.6)	3.116 (14.6)	4.600 (0.6)	6.593 14.8	9.282 30.9	13.039 49.1	
			10°	Log. spiral } $K_{PE}$ ----- method $\omega_0$ (34.4) Sokolovski } $K_{PE}$ 1.601		-----	1.623 (34.4)	2.706 (18.0)	4.201 (3.0)	6.246 11.4	9.046 26.6	12.980 42.9
	20°	Log. spiral } $K_{PE}$ ----- method $\omega_0$ ----- Sokolovski } $K_{PE}$ -----		-----	2.191 (22.6)	3.724 (6.5)	5.829 8.2	8.754 23.0	12.916 38.6			
		30°	Log. spiral } $K_{PE}$ ----- method $\omega_0$ ----- Sokolovski } $K_{PE}$ -----		-----	1.079 (37.6)	3.075 (11.4)	5.285 4.3	8.363 19.6	12.801 34.8		
$\phi=42.5^\circ$	$\delta=0^\circ$	$\alpha_1=0^\circ$	0°	Log. spiral } $K_{PE}$ 1.334 method $\omega_0$ (44.5) Sokolovski } $K_{PE}$ 1.306		2.205 (28.5)	3.433 (14.1)	5.260 (0.5)	7.593 14.5	11.011 29.9	15.991 47.1	
			10°	Log. spiral } $K_{PE}$ ----- method $\omega_0$ (32.1) Sokolovski } $K_{PE}$ 1.784		-----	1.795 (32.1)	3.010 (16.9)	4.746 (2.7)	7.222 11.5	10.767 26.3	15.980 42.1
	20°	Log. spiral } $K_{PE}$ ----- method $\omega_0$ (39.5) Sokolovski } $K_{PE}$ 1.195		-----	1.208 (39.5)	2.495 (20.7)	4.250 (5.7)	6.782 8.6	10.468 23.1	15.965 38.3		
		30°	Log. spiral } $K_{PE}$ ----- method $\omega_0$ ----- Sokolovski } $K_{PE}$ -----		-----	1.693 (27.7)	3.594 1.689	6.216 5.4	10.070 20.0	15.907 35.1		
$\phi=45.0^\circ$	$\delta=0^\circ$	$\alpha_1=0^\circ$	0°	Log. spiral } $K_{PE}$ 1.449 method $\omega_0$ (42.4) Sokolovski } $K_{PE}$ 2.390		2.402 (27.4)	3.792 (13.6)	5.829 0.3	8.808 14.0	13.202 29.0	19.904 45.6	
			10°	Log. spiral } $K_{PE}$ ----- method $\omega_0$ (30.4) Sokolovski } $K_{PE}$ 1.981		-----	1.992 (30.4)	3.355 (16.0)	5.385 (2.4)	8.412 11.5	12.955 26.0	19.966 41.4
	20°	Log. spiral } $K_{PE}$ ----- method $\omega_0$ ----- Sokolovski } $K_{PE}$ -----		-----	1.449 (35.2)	2.833 (19.0)	4.867 (5.0)	7.947 9.0	12.652 23.3	20.029 38.2		
		30°	Log. spiral } $K_{PE}$ ----- method $\omega_0$ ----- Sokolovski } $K_{PE}$ -----		-----	2.090 (24.0)	4.198 2.086	7.354 6.2	12.251 20.6	20.061 35.3		





TABLE A-4 (4). Values of  $K_{PE}$  and  $\omega_0$  of the spiral method and the Sokolovski method for various values of  $\beta$  in the case of  $\alpha_1=0^\circ$ ,  $\delta=1/2\cdot\phi$  and  $\phi=35^\circ\sim 45^\circ$ 

$\phi$	$\delta$	$\alpha_1$	$\theta_0$	KPE		$\beta$	-30°	-20°	-10°	0°	10°	20°	30°	
				$\omega_0$ (degrees)										
$\phi=35.0^\circ$	$\delta=1/2\cdot\phi$	$\alpha_1=0^\circ$	0°	Log. spiral method	KPE	-----	2.464	4.038	6.220	9.040	12.640	17.188		
				Sokolovski	KPE	-----	(4.0)	11.5	25.7	40.5	56.2	75.6		
			10°	Log. spiral method	KPE	-----	1.743	3.330	5.520	8.412	12.205	17.155		
				Sokolovski	KPE	-----	(11.8)	6.6	21.5	36.1	50.9	67.0		
20°	Log. spiral method	KPE	-----	-----	2.418	4.667	7.650	11.638	16.985					
	Sokolovski	KPE	-----	-----	(0.8)	16.8	31.7	46.5	61.5					
30°	Log. spiral method	KPE	-----	-----	-----	3.432	6.632	10.863	16.648					
	Sokolovski	KPE	-----	-----	-----	9.4	26.8	42.1	57.1					
$\phi=37.5^\circ$	$\delta=1/2\cdot\phi$	$\alpha_1=0^\circ$	0°	Log. spiral method	KPE	1.503	2.849	4.736	7.469	11.164	16.092	22.603		
				Sokolovski	KPE	(20.1)	(1.9)	12.9	26.8	40.8	56.0	73.6		
			10°	Log. spiral method	KPE	-----	2.109	3.960	6.674	10.435	15.592	22.620		
				Sokolovski	KPE	-----	(7.9)	8.7	23.1	37.2	51.4	66.8		
20°	Log. spiral method	KPE	-----	-----	2.983	5.724	9.562	14.948	22.490					
	Sokolovski	KPE	-----	-----	2.9	18.9	33.5	47.8	62.2					
30°	Log. spiral method	KPE	-----	-----	-----	4.420	8.419	14.075	22.183					
	Sokolovski	KPE	-----	-----	-----	12.9	29.1	43.9	58.4					
$\phi=40.0^\circ$	$\delta=1/2\cdot\phi$	$\alpha_1=0^\circ$	0°	Log. spiral method	KPE	1.754	3.211	5.613	9.089	14.012	20.882	30.377		
				Sokolovski	KPE	(16.4)	0.3	14.2	27.6	41.4	56.1	72.5		
			10°	Log. spiral method	KPE	-----	2.533	4.750	8.174	13.157	20.308	30.493		
				Sokolovski	KPE	-----	(4.8)	10.5	24.4	38.2	52.2	67.1		
20°	Log. spiral method	KPE	-----	1.094	3.700	7.099	12.144	19.573	30.451					
	Sokolovski	KPE	-----	(21.2)	5.9	20.9	35.0	48.8	63.2					
30°	Log. spiral method	KPE	-----	-----	1.611	5.675	10.838	18.584	30.223					
	Sokolovski	KPE	-----	-----	(9.2)	16.1	31.1	45.6	59.8					
$\phi=42.5^\circ$	$\delta=1/2\cdot\phi$	$\alpha_1=0^\circ$	0°	Log. spiral method	KPE	2.045	3.769	6.732	11.234	17.923	27.709	41.887		
				Sokolovski	KPE	(13.3)	2.0	15.4	28.7	42.5	56.5	71.9		
			10°	Log. spiral method	KPE	-----	1.258	3.043	5.758	10.166	16.906	27.052	42.190	
				Sokolovski	KPE	-----	(21.9)	(2.1)	12.4	25.8	39.3	53.1	67.5	
20°	Log. spiral method	KPE	-----	1.893	4.603	8.927	15.713	26.212	42.321					
	Sokolovski	KPE	-----	(9.7)	8.4	22.6	36.4	50.3	64.1					
30°	Log. spiral method	KPE	-----	-----	2.893	7.330	14.195	25.086	42.261					
	Sokolovski	KPE	-----	-----	0.8	18.6	33.2	47.2	61.3					
$\phi=45.0^\circ$	$\delta=1/2\cdot\phi$	$\alpha_1=0^\circ$	0°	Log. spiral method	KPE	2.388	4.466	8.189	14.139	23.442	37.750	59.537		
				Sokolovski	KPE	(10.8)	3.6	16.6	29.7	43.0	56.8	71.8		
			10°	Log. spiral method	KPE	-----	1.605	3.550	7.072	12.873	22.215	37.003	60.187	
				Sokolovski	KPE	-----	(16.6)	0.4	14.0	27.2	40.5	54.0	68.0	
20°	Log. spiral method	KPE	-----	2.505	5.772	11.419	20.785	36.046	60.650					
	Sokolovski	KPE	-----	(5.4)	10.6	24.6	38.0	51.5	65.2					
30°	Log. spiral method	KPE	-----	-----	3.997	9.584	18.987	34.760	60.927					
	Sokolovski	KPE	-----	-----	5.2	21.2	35.2	49.0	62.7					

TABLE A-4 (5). Values of  $K_{PE}$  and  $\omega_0$  of the spiral method and the Sokolovski method for various values of  $\beta$  in the case of  $\alpha_1=0^\circ$ ,  $\delta=2/3\cdot\phi$  and  $\phi=20^\circ \sim 32.5^\circ$

$\phi$	$\delta$	$\alpha_1$	$\theta_0$	$K_{PE}$ $\omega_0$ (degrees)	$\beta$	-50°	-20°	-10°	0°	10°	20°	30°
$\phi=20.0^\circ$	$\delta=2/3\cdot\phi$	$\alpha_1=0^\circ$	0°	Log. spiral } $K_{PE}$ method } $\omega_0$ Sokolovski } $K_{PE}$	-----	-----	1.862	2.660	3.425	-----	-----	-----
				-----	-----	7.7	26.8	46.7	-----	-----		
			10°	Log. spiral } $K_{PE}$ method } $\omega_0$ Sokolovski } $K_{PE}$	-----	-----	1.052	2.221	3.102	3.966	4.783	
				-----	-----	(22.0)	16.9	36.0	56.1	94.8		
20°	Log. spiral } $K_{PE}$ method } $\omega_0$ Sokolovski } $K_{PE}$	-----	-----	-----	1.236	2.639	3.659	4.684				
	-----	-----	-----	1.236	25.7	45.0	65.5					
30°	Log. spiral } $K_{PE}$ method } $\omega_0$ Sokolovski } $K_{PE}$	-----	-----	-----	-----	1.474	3.162	4.414				
	-----	-----	-----	-----	2.8	34.5	54.2					
$\phi=22.5^\circ$	$\delta=2/3\cdot\phi$	$\alpha_1=0^\circ$	0°	Log. spiral } $K_{PE}$ method } $\omega_0$ Sokolovski } $K_{PE}$	-----	1.232	2.131	3.070	4.030	5.000	-----	
				-----	-----	(15.5)	10.4	27.9	45.9	70.3	-----	
			10°	Log. spiral } $K_{PE}$ method } $\omega_0$ Sokolovski } $K_{PE}$	-----	-----	1.506	2.597	3.663	4.776	5.914	
				-----	-----	(3.0)	19.6	37.1	55.5	80.3		
20°	Log. spiral } $K_{PE}$ method } $\omega_0$ Sokolovski } $K_{PE}$	-----	-----	-----	1.855	3.162	4.429	5.784				
	-----	-----	-----	7.0	28.6	46.3	65.1					
30°	Log. spiral } $K_{PE}$ method } $\omega_0$ Sokolovski } $K_{PE}$	-----	-----	-----	-----	2.293	3.894	5.487				
	-----	-----	-----	-----	16.0	37.6	55.7					
$\phi=25.0^\circ$	$\delta=2/3\cdot\phi$	$\alpha_1=0^\circ$	0°	Log. spiral } $K_{PE}$ method } $\omega_0$ Sokolovski } $K_{PE}$	-----	1.470	2.449	3.568	4.778	6.072	-----	
				-----	-----	(8.2)	12.6	28.9	45.8	66.5	-----	
			10°	Log. spiral } $K_{PE}$ method } $\omega_0$ Sokolovski } $K_{PE}$	-----	-----	1.816	3.051	4.362	5.804	7.372	
				-----	-----	-----	2.9	21.8	38.3	55.4	76.5	
20°	Log. spiral } $K_{PE}$ method } $\omega_0$ Sokolovski } $K_{PE}$	-----	-----	-----	2.318	3.811	5.412	7.217				
	-----	-----	-----	-----	12.3	31.0	47.7	65.0				
30°	Log. spiral } $K_{PE}$ method } $\omega_0$ Sokolovski } $K_{PE}$	-----	-----	-----	-----	2.950	4.828	6.893				
	-----	-----	-----	-----	21.3	40.2	57.1					
$\phi=27.5^\circ$	$\delta=2/3\cdot\phi$	$\alpha_1=0^\circ$	0°	Log. spiral } $K_{PE}$ method } $\omega_0$ Sokolovski } $K_{PE}$	-----	1.720	2.829	4.180	5.719	7.446	-----	
				-----	-----	(3.5)	14.5	30.0	46.0	64.4	-----	
			10°	Log. spiral } $K_{PE}$ method } $\omega_0$ Sokolovski } $K_{PE}$	-----	-----	2.178	3.610	5.243	7.130	9.290	
				-----	-----	-----	6.9	23.9	39.4	55.6	74.4	
20°	Log. spiral } $K_{PE}$ method } $\omega_0$ Sokolovski } $K_{PE}$	-----	-----	-----	2.848	4.631	6.685	9.116				
	-----	-----	-----	-----	16.1	33.1	49.0	65.4				
30°	Log. spiral } $K_{PE}$ method } $\omega_0$ Sokolovski } $K_{PE}$	-----	-----	-----	-----	3.731	6.040	8.766				
	-----	-----	-----	-----	25.3	42.5	58.6					
$\phi=30.0^\circ$	$\delta=2/3\cdot\phi$	$\alpha_1=0^\circ$	0°	Log. spiral } $K_{PE}$ method } $\omega_0$ Sokolovski } $K_{PE}$	-----	1.923	3.289	4.943	6.917	9.237	-----	
				-----	-----	0.6	16.4	31.0	46.2	63.4	-----	
			10°	Log. spiral } $K_{PE}$ method } $\omega_0$ Sokolovski } $K_{PE}$	-----	-----	2.600	4.307	6.370	8.868	11.862	
				-----	-----	-----	10.0	25.8	40.6	56.2	73.4	
20°	Log. spiral } $K_{PE}$ method } $\omega_0$ Sokolovski } $K_{PE}$	-----	-----	1.257	3.490	5.682	8.362	11.676				
	-----	-----	-----	(9.2)	19.2	35.2	50.4	66.2				
30°	Log. spiral } $K_{PE}$ method } $\omega_0$ Sokolovski } $K_{PE}$	-----	-----	-----	1.688	4.712	7.643	11.306				
	-----	-----	-----	-----	1.6	28.6	44.6	60.2				
$\phi=32.5^\circ$	$\delta=2/3\cdot\phi$	$\alpha_1=0^\circ$	0°	Log. spiral } $K_{PE}$ method } $\omega_0$ Sokolovski } $K_{PE}$	-----	2.247	3.856	5.908	8.471	11.619	15.368	
				-----	-----	3.3	18.2	32.3	46.7	62.8	84.1	
			10°	Log. spiral } $K_{PE}$ method } $\omega_0$ Sokolovski } $K_{PE}$	-----	-----	1.510	3.111	5.188	7.838	11.189	
				-----	-----	-----	(7.3)	12.7	27.6	41.9	56.7	73.0
20°	Log. spiral } $K_{PE}$ method } $\omega_0$ Sokolovski } $K_{PE}$	-----	-----	2.042	4.294	7.055	10.610	15.201				
	-----	-----	-----	3.4	22.1	37.2	51.9	66.9				
30°	Log. spiral } $K_{PE}$ method } $\omega_0$ Sokolovski } $K_{PE}$	-----	-----	-----	2.883	5.985	9.801	14.819				
	-----	-----	-----	-----	12.8	31.5	46.8	61.9				

TABLE A-4 (6). Values of  $K_{PE}$  and  $\omega_0$  of the spiral method and the Sokolovski method for various values of  $\beta$  in the case of  $\alpha_1=0^\circ$ ,  $\delta=2/3\cdot\phi$  and  $\phi=35^\circ\sim 45^\circ$ 

$\phi$	$\delta$	$\beta$	$\theta_0$	$K_{PE}$		$\beta$	$-30^\circ$	$-20^\circ$	$-10^\circ$	$0^\circ$	$10^\circ$	$20^\circ$	$30^\circ$
				Log. spiral method	Sokolovski								
$\phi=35.0^\circ$	$\delta=2/3\cdot\phi$	$\alpha_1=0^\circ$	$0^\circ$	Log. spiral method	$K_{PE}$	-----	2.634	4.563	7.147	10.523	14.853	20.276	
				Sokolovski	$K_{PE}$	-----	5.8	19.7	33.5	47.5	62.6	81.0	
				Log. spiral method	$\omega_0$	-----	1.910	3.744	6.324	9.782	14.352	20.323	
				Sokolovski	$K_{PE}$	-----	(2.0)	15.2	29.3	43.3	57.5	73.0	
$\phi=35.0^\circ$	$\delta=2/3\cdot\phi$	$\alpha_1=0^\circ$	$20^\circ$	Log. spiral method	$K_{PE}$	-----	-----	2.663	5.325	8.880	13.687	20.162	
				Sokolovski	$\omega_0$	-----	-----	8.2	24.6	39.1	53.3	67.7	
				Log. spiral method	$K_{PE}$	-----	-----	-----	3.883	7.676	12.769	19.787	
				Sokolovski	$\omega_0$	-----	-----	-----	17.6	34.2	48.9	63.3	
$\phi=37.5^\circ$	$\delta=2/3\cdot\phi$	$\alpha_1=0^\circ$	$0^\circ$	Log. spiral method	$K_{PE}$	1.646	3.107	5.462	8.768	13.289	19.348	27.301	
				Sokolovski	$\omega_0$	(8.9)	7.9	21.5	34.8	48.2	62.8	79.6	
				Log. spiral method	$K_{PE}$	-----	2.257	4.545	7.815	12.413	18.765	27.425	
				Sokolovski	$K_{PE}$	-----	2.5	17.5	31.1	44.6	58.4	73.2	
$\phi=37.5^\circ$	$\delta=2/3\cdot\phi$	$\alpha_1=0^\circ$	$20^\circ$	Log. spiral method	$K_{PE}$	-----	-----	3.395	6.679	11.360	17.997	27.326	
				Sokolovski	$\omega_0$	-----	-----	11.7	27.1	41.1	54.8	68.8	
				Log. spiral method	$K_{PE}$	-----	-----	-----	5.122	9.979	16.945	26.996	
				Sokolovski	$\omega_0$	-----	-----	-----	21.3	36.9	51.1	65.0	
$\phi=40.0^\circ$	$\delta=2/3\cdot\phi$	$\alpha_1=0^\circ$	$0^\circ$	Log. spiral method	$K_{PE}$	1.960	3.696	6.624	10.935	17.110	25.764	37.662	
				Sokolovski	$\omega_0$	(5.4)	9.9	23.0	36.0	49.2	63.1	78.9	
				Log. spiral method	$K_{PE}$	-----	2.780	5.581	9.814	16.060	25.086	37.942	
				Sokolovski	$K_{PE}$	-----	5.5	19.5	32.8	46.0	59.4	73.7	
$\phi=40.0^\circ$	$\delta=2/3\cdot\phi$	$\alpha_1=0^\circ$	$20^\circ$	Log. spiral method	$K_{PE}$	-----	1.206	4.316	8.497	14.811	24.196	37.976	
				Sokolovski	$\omega_0$	-----	(10.2)	14.9	29.3	42.8	56.2	70.0	
				Log. spiral method	$K_{PE}$	-----	-----	1.794	6.755	13.197	22.982	37.760	
				Sokolovski	$\omega_0$	-----	-----	0.4	24.7	39.3	53.0	66.8	
$\phi=42.5^\circ$	$\delta=2/3\cdot\phi$	$\alpha_1=0^\circ$	$0^\circ$	Log. spiral method	$K_{PE}$	2.336	4.446	8.159	13.903	22.531	35.204	53.468	
				Sokolovski	$\omega_0$	(2.5)	11.8	24.6	37.3	50.1	63.9	78.5	
				Log. spiral method	$K_{PE}$	1.405	3.433	6.951	12.561	21.253	34.418	54.042	
				Sokolovski	$\omega_0$	(10.5)	8.0	21.6	34.6	47.5	60.7	74.5	
$\phi=42.5^\circ$	$\delta=2/3\cdot\phi$	$\alpha_1=0^\circ$	$20^\circ$	Log. spiral method	$K_{PE}$	-----	2.070	5.521	11.003	19.744	33.383	54.341	
				Sokolovski	$\omega_0$	-----	0.6	17.8	31.4	44.6	57.9	71.3	
				Log. spiral method	$K_{PE}$	-----	-----	3.417	8.995	17.819	31.973	54.373	
				Sokolovski	$\omega_0$	-----	-----	10.4	27.6	41.6	55.0	68.5	
$\phi=45.0^\circ$	$\delta=2/3\cdot\phi$	$\alpha_1=0^\circ$	$0^\circ$	Log. spiral method	$K_{PE}$	2.565	5.419	10.238	18.080	30.470	49.587	78.527	
				Sokolovski	$\omega_0$	(0.6)	13.6	26.0	38.5	51.2	64.6	78.8	
				Log. spiral method	$K_{PE}$	1.848	4.276	8.810	16.440	28.883	48.684	79.654	
				Sokolovski	$\omega_0$	(5.6)	10.4	23.4	36.2	48.9	61.8	75.2	
$\phi=45.0^\circ$	$\delta=2/3\cdot\phi$	$\alpha_1=0^\circ$	$20^\circ$	Log. spiral method	$K_{PE}$	-----	2.846	7.151	14.555	27.024	47.484	80.470	
				Sokolovski	$\omega_0$	-----	5.0	20.2	33.6	46.6	59.5	72.6	
				Log. spiral method	$K_{PE}$	-----	-----	4.894	12.174	24.675	45.840	81.014	
				Sokolovski	$\omega_0$	-----	-----	14.8	30.2	43.8	57.0	70.1	

TABLE A-5. Values of  $K_{PE}$  and  $\omega_0$  of the spiral method and the Sokolovski method in the case of  $\alpha_1 = \beta = 0^\circ$  and  $\delta = -1/2 \cdot \phi$

$\theta_0$	KPE		$\phi$	20.0°	22.5°	25.0°	27.5°	30.0°	32.5°	35.0°	37.5°	40.0°	42.5°	45.0°
	$\omega_0$ (degrees)	method												
-30°	Log. spiral}	KPE	-----	-----	-----	-----	-----	2.071	2.128	2.190	2.247	2.298	2.344	2.383
	method	$\omega_0$	-----	-----	-----	-----	-----	9.2	(5.9)	(11.6)	(15.9)	(19.2)	(22.1)	(24.4)
-20°	Sokolovski	KPE	-----	-----	-----	-----	-----	2.005	2.068	2.129	2.186	2.239	2.287	2.330
	Log. spiral}	KPE	-----	-----	-----	-----	-----	(14.2)	(17.8)	(19.8)	(22.1)	(24.0)	(25.9)	(27.4)
-10°	method	$\omega_0$	-----	-----	-----	-----	-----	1.998	2.058	2.113	2.166	2.213	2.256	2.294
	Sokolovski	KPE	-----	-----	-----	-----	-----	1.869	1.935	2.004	2.104	2.160	2.213	2.262
0°	Log. spiral}	KPE	1.644	1.714	1.782	1.850	1.916	1.981	1.981	2.044	2.104	2.160	2.213	2.262
	method	$\omega_0$	(12.3)	(15.3)	(17.8)	(19.7)	(21.6)	(23.5)	(23.5)	(24.8)	(26.1)	(27.4)	(28.7)	(29.8)
10°	Sokolovski	KPE	1.642	1.710	1.776	1.842	1.905	1.967	1.967	2.026	2.083	2.136	2.185	2.230
	Log. spiral}	KPE	-----	-----	-----	-----	-----	1.803	1.871	1.938	2.003	2.065	2.124	2.180
20°	method	$\omega_0$	(24.3)	(25.1)	(25.8)	(26.5)	(27.4)	(28.1)	(28.1)	(28.8)	(29.5)	(30.2)	(30.9)	(31.6)
	Sokolovski	KPE	1.520	1.588	1.656	1.723	1.790	1.856	1.856	1.921	1.983	2.043	2.100	2.153
30°	Log. spiral}	KPE	1.351	1.428	1.504	1.580	1.656	1.731	1.731	1.805	1.877	1.947	2.015	2.080
	method	$\omega_0$	(36.1)	(34.7)	(33.8)	(33.1)	(32.8)	(32.7)	(32.7)	(32.8)	(32.9)	(33.0)	(33.3)	(33.6)
20°	Sokolovski	KPE	1.341	1.417	1.493	1.568	1.642	1.716	1.716	1.788	1.859	1.928	1.995	2.058
	Log. spiral}	KPE	0.906	1.130	1.247	1.348	1.443	1.534	1.554	1.623	1.709	1.792	1.873	1.950
30°	method	$\omega_0$	(66.9)	(49.9)	(44.8)	(41.7)	(39.6)	(38.1)	(38.1)	(37.2)	(36.5)	(36.0)	(35.7)	(35.6)
	Sokolovski	KPE	1.112	1.112	1.232	1.335	1.430	1.521	1.521	1.608	1.694	1.776	1.856	1.933
30°	Log. spiral}	KPE	-----	-----	-----	-----	-----	0.883	1.177	1.523	1.447	1.559	1.665	1.765
	method	$\omega_0$	-----	-----	-----	-----	-----	(47.0)	(47.9)	(44.0)	(41.7)	(40.0)	(38.9)	(38.0)
Sokolovski	KPE	-----	-----	-----	-----	-----	-----	1.164	1.311	1.435	1.548	1.653	1.753	



TABLE A-6 (2). Values of  $K_{PE}$  and  $\omega_0$  of the spiral method and the Sokolovski method for various values of  $\alpha_1$  in the case of  $\delta=\phi$ ,  $\beta=0^\circ$  and  $\phi=30^\circ$ ,  $32.5^\circ$

$\phi$	$\delta$	$\beta$	$\theta_0$	$K_{PE}$		$\alpha_1$	$-70^\circ$	$-60^\circ$	$-50^\circ$	$-40^\circ$	$-30^\circ$	$-20^\circ$	$-10^\circ$	$0^\circ$	$10^\circ$	$20^\circ$	$30^\circ$												
				$\omega_0$ (degrees)	$\omega_0$																								
$\phi=30.0^\circ$	$-30^\circ$	KPE method	Sokolovski	Log. spiral method	KPE	125.806 147.4	68.642 134.8	42.301 123.4	27.900 112.6	19.264 102.4	13.783 92.8	10.154 83.6	7.640 74.4	5.850 65.4	4.547 56.6	3.578 48.0													
																	Log. spiral method	KPE	119.769	64.936	39.707	26.021	17.889	12.775	9.409	7.087	5.438	4.240	3.350
	Log. spiral method	KPE	108.745	59.295	36.637	24.393	17.026	12.039	9.142	6.937	5.359	4.200	3.090																
														Sokolovski	KPE	109.282	59.042	36.010	23.562	16.194	11.579	8.549	6.438	4.974	3.894	24.2			
																											Sokolovski	KPE	116.2
	$0^\circ$	KPE method	Sokolovski	117.083	53.050	32.896	21.939	15.360	11.142	8.305	6.328	4.907	3.863	2.803															
															Sokolovski	KPE	97.480	52.518	31.969	20.900	14.371	10.296	7.626	5.783	4.472	3.517	2.803		
																												Sokolovski	KPE
$10^\circ$	KPE method	Sokolovski	84.962	46.547	28.947	19.370	13.610	9.911	7.418	5.675	4.420	3.494	2.467																
														Sokolovski	KPE	83.756	44.998	27.342	17.866	12.297	8.836	6.574	5.010	3.895	3.079	2.467			
																											Sokolovski	KPE	104.0
$20^\circ$	KPE method	Sokolovski	71.450	39.282	24.512	16.486	11.640	8.518	6.408	4.928	3.858	3.064	2.024																
														Sokolovski	KPE	66.193	35.432	21.482	14.030	9.677	6.990	5.239	4.024	3.153	2.510	2.024			
																											Sokolovski	KPE	96.6
$30^\circ$	KPE method	Sokolovski	59.292	30.256	19.013	12.881	9.164	6.759	5.128	3.970	3.131	2.503	1.000																
														Sokolovski	KPE	15.441	9.253	6.012	4.173	3.077	2.376	1.878	1.508	1.225	5.8	(59.4)			
																											Sokolovski	KPE	75.8
$\phi=32.5^\circ$	$-30^\circ$	KPE method	Sokolovski	Log. spiral method	KPE	195.380 135.5	102.957 123.9	61.177 113.1	38.928 102.7	25.960 92.7	17.959 83.3	12.808 73.9	9.346 64.7	6.954 55.9	5.261 47.1	4.037 38.5													
																	Log. spiral method	KPE	182.854	95.827	56.671	35.936	23.915	16.536	11.802	8.628	6.436	4.886	3.765
	Log. spiral method	KPE	165.461	87.062	52.015	33.447	22.597	15.832	11.412	8.417	6.327	4.833	3.475																
														Sokolovski	KPE	167.367	87.430	51.581	32.660	21.725	15.033	10.750	7.878	5.896	4.492	3.475			
																											Sokolovski	KPE	117.7
	$0^\circ$	KPE method	Sokolovski	148.724	78.365	46.900	30.219	14.378	10.395	7.692	5.803	4.450	3.163																
														Sokolovski	KPE	150.278	78.299	46.110	29.167	19.403	13.444	9.638	7.086	5.322	4.071	3.163			
																											Sokolovski	KPE	112.5
$10^\circ$	KPE method	Sokolovski	131.458	69.389	41.608	26.874	18.250	12.861	9.329	7.374	5.247	4.039	2.803																
														Sokolovski	KPE	130.670	67.910	39.924	25.236	16.796	11.662	8.390	6.194	4.673	3.592	2.803			
																											Sokolovski	KPE	107.4
$20^\circ$	KPE method	Sokolovski	112.386	59.454	35.752	23.164	15.786	11.168	8.136	6.069	4.617	3.569	2.347																
														Sokolovski	KPE	106.147	54.997	32.268	20.384	13.583	9.465	6.847	5.087	3.864	2.989	2.347			
																											Sokolovski	KPE	101.5
$30^\circ$	KPE method	Sokolovski	89.208	47.374	28.610	18.631	12.767	9.086	6.660	5.000	3.827	2.976	1.605																
														Sokolovski	KPE	67.933	34.990	20.451	12.906	8.629	6.067	4.450	3.354	2.583	2.024	1.605			
																											Sokolovski	KPE	90.8









TABLE A-7. Percent difference of  $K_{PE}$  of the Sokolovski method for various numbers of division of  $(\alpha_2 - \alpha_1)$  in the case of  $\delta = 1/2 \cdot \phi = 20^\circ$

Numbers of division	$S_0, K_{PE}$	$\alpha_2 - \alpha_1$		54.5°	58.9°	65.0°	75.5°	84.5°	95.0°	105.5°	115.5°	135.5°
		$\alpha_1, \beta, \theta_0$		$\alpha_1=0^\circ$ $\beta=0^\circ$ $\theta_0=30^\circ$	$\alpha_1=0^\circ$ $\beta=0^\circ$ $\theta_0=20^\circ$	$\alpha_1=0^\circ$ $\beta=0^\circ$ $\theta_0=0^\circ$	$\alpha_1=0^\circ$ $\beta=0^\circ$ $\theta_0=-30^\circ$	$\alpha_1=-30^\circ$ $\beta=0^\circ$ $\theta_0=30^\circ$	$\alpha_1=-30^\circ$ $\beta=0^\circ$ $\theta_0=0^\circ$	$\alpha_1=-30^\circ$ $\beta=0^\circ$ $\theta_0=-30^\circ$	$\alpha_1=-20^\circ$ $\beta=0^\circ$ $\theta_0=-10^\circ$	$\alpha_1=-30^\circ$ $\beta=0^\circ$ $\theta_0=0^\circ$
1000	$S_0$			3.524	4.783	6.516	7.211	9.836	19.143	21.705	31.353	65.740
	$K_{PE}$			5.674	7.098	9.086	11.611	18.288	30.823	40.355	47.243	105.852
4000 ~ 6000	$S_0$			3.524	4.783	6.514	7.205	9.826	19.110	21.647	* 31.243	** 65.334
	$K_{PE}$			5.674	7.098	9.083	11.601	18.269	30.770	40.247	47.077	105.198
Error (%)				0.00	0.00	0.04	0.08	0.10	0.17	0.27	0.35	0.62

\* : 5000 segments  
\*\* : 6000 segments

TABLE A-8. Percent difference of  $K_{PE}$  of the Sokolovski method for  $\Delta\omega' = 0.001^\circ$  in the case of  $\delta = \phi = 30^\circ$ ,  $\theta_0 = 20^\circ$  and  $\beta = 0^\circ$

$\Delta\omega$	$K_{PE}$ Error	$\alpha_1$		-70°	-60°	-40°	-20°	0°	20°
1°	$K_{PE}$			53.649	29.699	12.651	6.638	3.895	2.446
	Error (%)			1.88	1.84	1.79	1.79	1.89	2.28
0.1°	$K_{PE}$			54.513	30.169	12.846	6.743	3.962	2.496
	Error (%)			0.30	0.29	0.27	0.24	0.20	0.28
0.001°	$K_{PE}$			54.678	30.256	12.881	6.759	3.970	2.503

TABLE A-9. Percent difference of  $K_{PE}$  of the spiral method for  $\Delta\omega = 0.01^\circ$  in the case of  $\delta = 1/2 \cdot \phi = 20^\circ$

$\alpha_2 - \alpha_1$	$\phi=40^\circ$ $\delta=20^\circ$	$\Delta\omega$	0.01°	0.02°	0.2°	1.0°
			$\alpha_1, \beta, \theta_0$			
130.0°	$\alpha_1=-20^\circ$ $\beta=20^\circ$ $\theta_0=-20^\circ$	$K_{PE}$	49.5275	49.5275	49.5281	49.5347
		Error (%)	0	0	0	0.01
102.0°	$\alpha_1=-20^\circ$ $\beta=20^\circ$ $\theta_0=30^\circ$	$K_{PE}$	41.0258	41.0258	41.0262	41.0297
		Error (%)	0	0	0	0.01
75.5°	$\alpha_1=0^\circ$ $\beta=0^\circ$ $\theta_0=0^\circ$	$K_{PE}$	11.6322	11.6322	11.6322	11.6334
		Error (%)	0	0	0	0.01
54.5°	$\alpha_1=0^\circ$ $\beta=0^\circ$ $\theta_0=30^\circ$	$K_{PE}$	5.6747	5.6747	5.6747	5.6753
		Error (%)	0	0	0	0.01